2016

Phosphorus removal using titanium dioxide nanoparticles in wastewater treatment

Suyoung Choi Mr.
choi8150@mylaurier.ca

Phosphorus Removal using TiO_2 Nanoparticles in Wastewater Treatment

Suyoung Choi

Bachelor of Science, Applied Chemistry, Korea Military Academy, 2008

THESIS

submitted to the Department of Chemistry

in partial fulfillment of the requirements for

the degree of Master of Science

Wilfrid Laurier University

Waterloo, Ontario, Canada

Abstract

Environmental issues have become a serious problem for the Republic of Korea Army. Especially, due to eutrophication, local surface water has been deteriorated for several years. Phosphorus is the main cause of eutrophication and excessive phosphorus can be found around many military garrison and camps. Thus, in this thesis, in order to remove excessive phosphorus in local fresh water, various size of titanium dioxide (TiO_2) such as bulk powder and nanoparticles were used with variation of several parameters such as pH or ionic strength of samples to optimize phosphorus removal in wastewater.

In the first investigation, TiO_2 bulk powder was used to determine optimal pH of phosphorus adsorption onto three types of TiO_2 bulk powder (particle size > 5μm). In terms of phosphorus removal, when pH increases removed phosphorus decreases. A percent phosphorus removal was 20% at pH 10 and 27% at pH 4, respectively. This pH dependence trend was observed for all three titanium species. Among three types of bulk powder (rutile, anatase, mixture), the mixture bulk powder showed maximum phosphorus removal, that was approximately 27% while anatase showed 21% and rutile showed 24%, respectively. To determine adsorption isotherms, Langmuir and Freudlich models were used. The experimental data was better fit by a Langmuir model compared

to a Freudlich model; Freudlich model actually had trends in the residuals because it cannot fit a saturable relationship. Based on the equation for Langmuir model, written as $X = \frac{C*LT*KL}{C*KL+1}$, binding capacity ($L_T$) and equilibrium adsorption constant K (K_L) for Langmuir model were 0.77mg/L and 1.03L/mg, respectively.

In the second investigation, advanced wastewater treatment system called Photo-Cat technology was used to remove phosphorus in synthetic wastewater and real wastewater sample using TiO_2 nanoparticles. In terms of pH dependence, inversed trend in comparison with the result of the first investigation was observed (i.e. greater phosphorus removal at high pH). The pH trend was due to the tap water used in the Photo-Cat system. The tap water in Photo-Cat system could remove phosphorus even without the addition of TiO_2 nanoparticles by precipitation at high pH (e.g. pH 10 of calcium phosphate). Also, the Photo-Cat system could remove even more phosphorus in synthetic wastewater sample by using TiO_2 nanoparticles. It is likely due to improved particle aggregation before nano filtration. In addition, using Photo-Cat system was expected to convert organic phosphorus into reactive phosphorus by irradiation of UV light. However, turning on UV light to synthetic wastewater samples including TiO_2 nanoparticles achieved no increased phosphorus removal. Using real wastewater sample, Photo-Cat system showed removal of total phosphorus (TP) by ceramic

membrane filter. However, the addition of TiO_2 nanoparticles and UV light could not show any additional removal.

In conclusion, phosphorus in wastewater can be removed using TiO_2 nanoparticles via Photo Cat system. However, the idea that irradiation of UV light can convert organic phosphorus into reactive phosphorus was demonstrated not to be efficient. Although UV light gave no additional phosphorus removal, the Photo Cat system could show certain amount of phosphorus removal under the specific dependent variables such as pH. Thus, under optimal condition, using Photo Cat system can be effective method to remove phosphorus in wastewater.

Acknowledgement

First and foremost, I would like to thank my wonderful supervisor Dr. Scott Smith for the support and guidance. Throughout two years of working in his lab, he has given me not only academic assists but also life essential advice. It was honored to work with him for my academic achievement. Thank to Dr. Vladimir Kitaev and Dr. Louise Dawe to be on my committee for spending their precious time graciously and giving me excellent advices.

I have to thank my lab mates who spent much time in Smith lab with me together. Rabia and Gisselle, your advice for my writing was really helpful. Holly and Farah, thanks to you, I could finish my experiment. Elissa and Mona, it was always good to have a chat with you guys.

I would like to thank my family for all the support. **현정아, 2년동안 나 챙기면서 준서까지 돌보느라 고생 많았어. 쉽지않은 타국생활 힘들었을텐데, 내색않고 잘 견뎌줘서 고마워. 사랑한다. 그리고 사랑하는 우리아들 준서야**, seeing your smiling face has always been my best moment. I love you two more than anyone can do. Also, **존경하는 양가 부모님, 항상 응원해 주셔서 감사드립니다. 부족한 아들이자 사위 항상 챙겨 주시고 격려해주시는 은혜 항상 기억하겠습니다. 그리고 동생 중범아, 언제나 묵묵하게 챙겨줘서 고맙다. 더 좋은 형**

이 될 수 있도록 노력하마.

Lastly, I have to thank Republic of Korea Army for financial support. After going back, I will serve as an honored military officer with all my devotion to my country.

Table of Contents

List of Figures

List of Tables

Chapter 1: Introduction

1.1 Overview

Approximately half of the global population is currently living in urban areas, with populations in these areas on the rise (Jutidamrongphan, 2012). For making urban areas more sustainable, segregation of reusable and recyclable natural resources (e.g. phosphorus, nitrogen) needs to become standard practice. Phosphorus and nitrogen are essential nutrients and have recycle system in nature, however, they have been disturbed by anthropogenic activities such as industrial and agricultural activities. (Jutidamrongphan, 2012). These activities bring about increases of phosphorus and due to this, phosphorus has been excessive in surface water and that has caused eutrophication (Jutidamrongphan, 2012; Chislock *et al*., 2013).

Due to water pollution (e.g. eutrophication), some countries like the Republic of Korea are facing water shortages in recent years. According to the Population Action International (PAI), the Republic of Korea is classified as a water-stressed country (Kim, 2003). Therefore, the development of efficient methods for the water reuse and recycling has become necessary (Kim, 2003).

Environmental issues have been treated as a serious problem which can fundamentally threaten the survival of a nation (Park, 2002). Thus, as concerns about the environment grow, the role and status of government has to be evolved to provide

increased protection of a citizen's right to live in environmentally safe conditions. Consequently, the Republic of Korea (ROK) Army's attitude toward environmental issues have been changed to protect and preserve the nation's natural resources and fulfill environmental security (Park, 2002).

In efforts to provide environmental security, the ROK Army made it mandatory for a battalion (consisting of > 400 soldiers) to install water sanitation facilities (Republic of Korea Army Headquarters, 1999). Accordingly, diverse kinds of sanitation facilities are now available for remediation of water pollution in the military (Park, 2002). However, the ROK Army is currently facing lack of sewage disposal and sanitation facilities which leads to some serious environmental problems, especially with water in regional streams or lakes (Kim *et al*., 2011). Thus, the ministry of national defense has recently decided to legislate several standards for prevention of environmental pollution, which include strict application of existing regulations and establishing new operations for environment protection (Ministry of National Defense, 2014).

1.2 Related Regulation of Wastewater and Actual Water Quality in the ROK Army

1.2.1 Standards of Facility of Wastewater Treatment

Standards for wastewater treatment facilities have been written based on the

statutes ‘the management and use of livestock excreta article No. 9 and No. 14’ (Water quality and aquatic ecosystem conservation act of 2014).

Based on the law of the management and use of livestock excreta Act No. 12516, article No. 14 (Water quality and aquatic ecosystem conservation act of 2014), an echelon that is over the size of an individual company class has to have a wastewater treatment facility or share a similar facility with a public wastewater treatment plant in cooperation with a local government (Republic of Korea Army Headquarters, 1999).

1.2.2 Effluent Quality Criteria of Wastewater

Due to deterioration of local lakes and rivers, wastewater quality criteria have become more rigorous over the past several years. Current wastewater quality criteria are shown in Table 1.1 in comparison with criteria of European Union (EU, Germany). In the Table 1.1, it is found that all criteria of Republic of Korea in terms of water quality have been stringent since 2013. Deterioration of water quality might be related to this criteria trend. Interestingly, except chemical oxygen demand (COD) level, all criteria for Republic of Korea are higher compared to criteria of Germany based on Table 1.1.

Many lakes and rivers have been a main source of potable water for local citizens. However, as mentioned above, the Republic of Korea has already been

classified as a water-stressed country (Kim, 2003). This means if the government does not improve current water quality, soon the nation will be facing a lack of drinking water due to poor water quality. Thus, the ministry of environment is forced to reform the bills that are related to environmental problems to prevent people from suffering from water related health problems (Lee et al., 2005).

Table 1.1: Water quality criteria for wastewater in the Republic of Korea and European Union (Adapted from water quality and aquatic ecosystem conservation Act No. 12519, article No.26, attached Table No.10; Republic of Korea. National Institute of Environmental Research, 2000).

Criteria	European Union (Germany)	2011	2012	2013-present
Biological Oxygen Demand (mg/L)	≤ 5	20	20	10
Chemical Oxygen Demand (mg/L)	≤ 20	40	40	20
Total Nitrogen (mg/L)	≤ 8	40	40	20
Total Phosphorus (mg/L)	≤ 0.3	4	4	2
Suspended Sludge (mg/L)	-	20	20	10

1.2.3 Present Water Quality of Environmental Facility in ROK Army

As water quality near military post and garrison have deteriorated since early

2000 (Park, 2002), the ROK Army is consistently trying to improve water quality in various ways (Ministry of National Defense, 2014), For this reason, some garrisons sometimes send their wastewater to garrisons that have their own purification facilities, which results in exceeding the wastewater capacities of said facilities (Republic of Korea Army Headquarters, 1999). Figure 1.1 shows that wastewater production of specific garrisons exceeds their daily treatment capacities (Park, 2002). For instance, the army training centre produces around 2500 tons of wastewater per day, however, their daily capacity for wastewater is only 1200 tons per day. If excess wastewater flows into local surface water (e.g. lake, river, and reservoir), it is likely to cause deterioration of water quality close to army facilities.

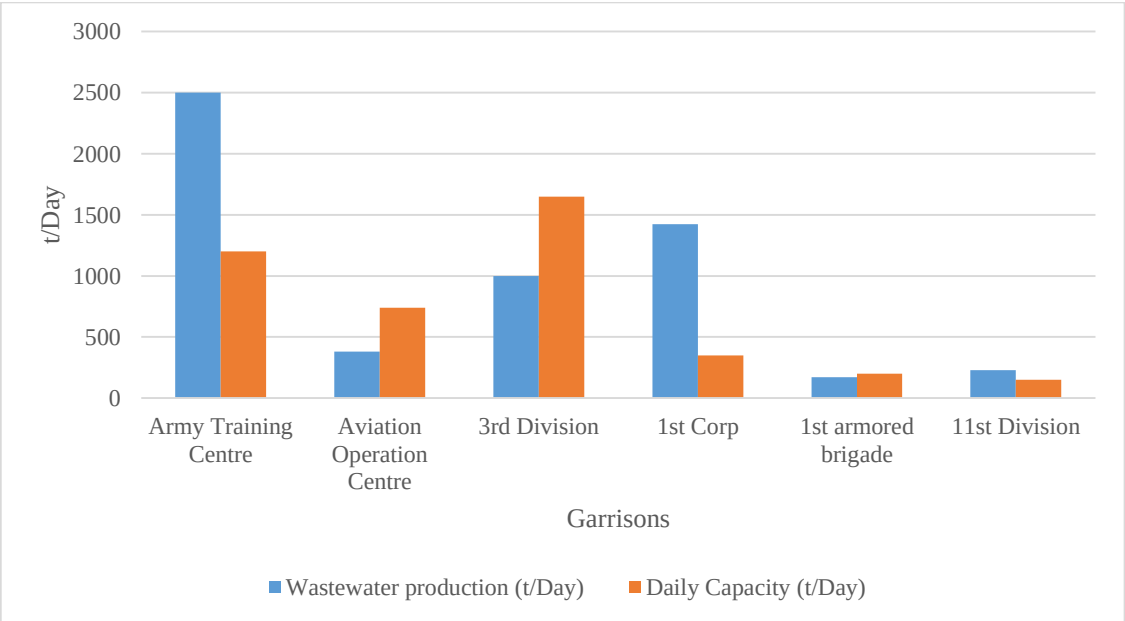

Figure 1.1: Comparison of wastewater production of the army echelon with daily capacity of wastewater production (Adapted from Park, 2002).

In Figure 1.2, similar trends in terms of water quality can be found. The

accepted maximum standards for both biological oxygen demand (BOD) and suspended sludge (SS) water quality are both 20 mg/L. However, approximately 70% of the ROK Army echelons are not able to meet the criteria in the Figure 1.2 (Park, 2002). For example, when it comes to BOD, only the army training centre and the 3rd division could meet the standard. As the data shown in Figure 1.2 were collected from all over the ROK, this can be considered a demonstration of the reality of water quality in the army.

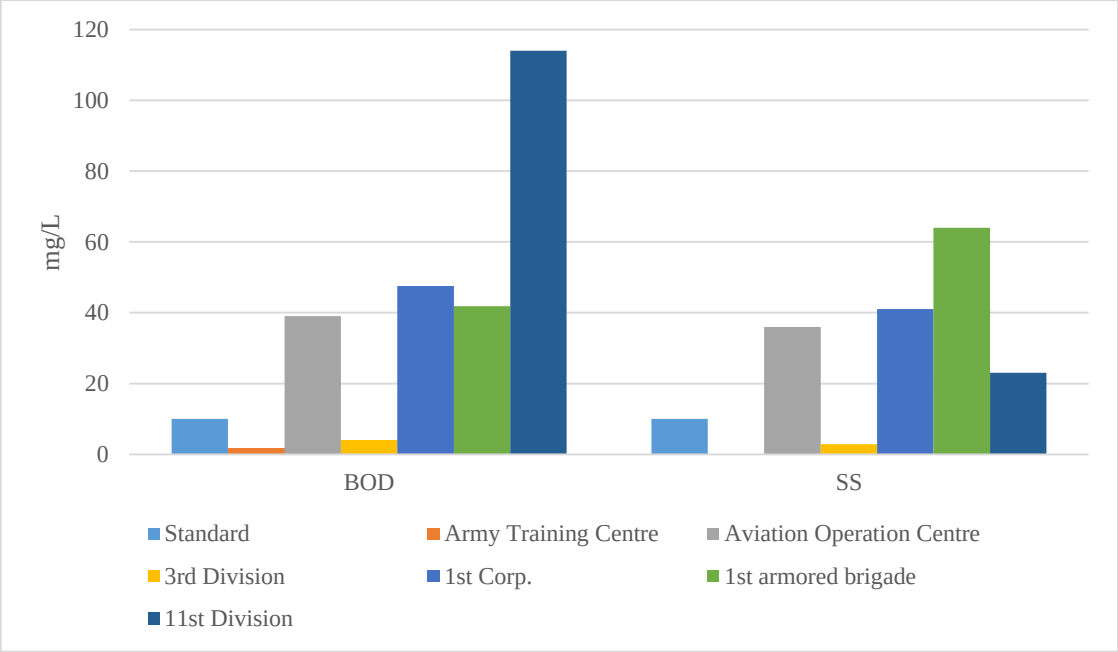

Figure 1.2: Actual effluent quality of diverse garrisons in the army (Adapted from Park, 2002). In this graph, the y axis represents unit of mg/L, while, the x axis represents biological oxygen demand (BOD) and suspended sludge (SS).

Figure 1.3 shows water quality of particular military echelons such as companies, battalions, and divisions. These three types of echelons are basic and

fundamental structures which comprise the ROK Army. Thus, the graph in Figure 1.3 can be considered the strongest evidence for indicating the ROK Army's current state in terms of water quality. According to Figure 1.3, most echelons exceed water quality standards. For example, accepted maximum biological oxygen demand (BOD) concentration is 10 mg/L, however, all echelons show more than 30 mg/L of BOD level. Similar trends can be found on other criteria like COD, total nitrogen (TN), and total phosphorus (TP).

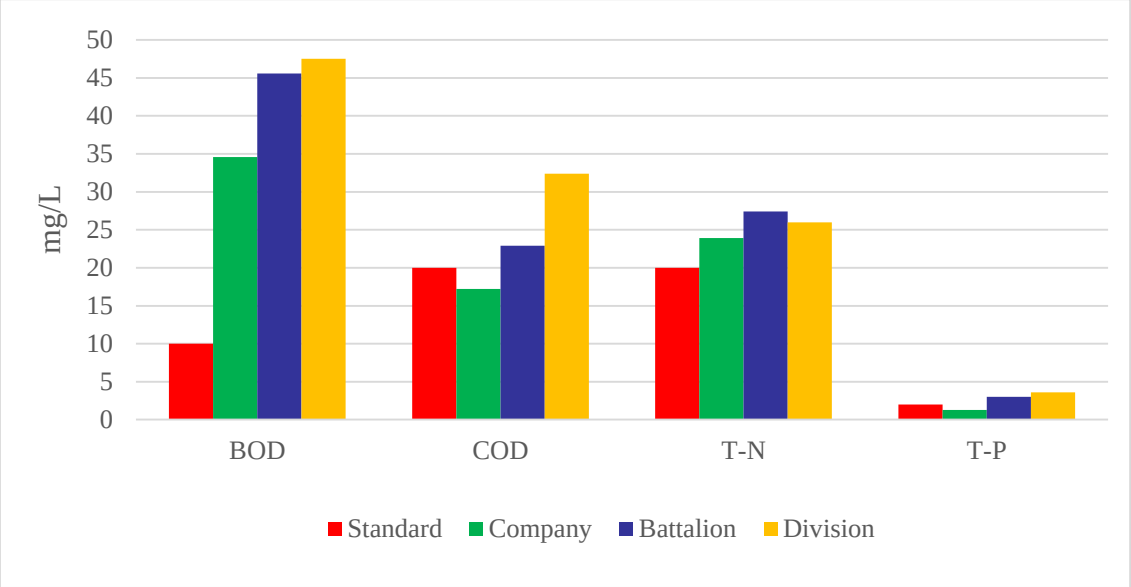

Figure 1.3: Several water quality criteria versus echelons; three types of echelons in the army exceed those criteria (Adapted from Park, 2002). In this graph, the y axis represents unit of mg/L, while, the x axis represents water quality criteria.

Due to environmental problems including water pollution as described above, the ROK Army has been dealing with several kinds of repercussions, including damage

compensation and penalties (Choi, 2001). For example, in Figure 1.4, officers from the ROK Marine 1st division are explaining in terms of illegal wastewater discharge into local stream and reimbursement for fishermen. Thus, for solving the series of problems described in this section, the ROK Army has to pay attention to the nations' voice in terms of environmental issues. It would be the fastest way to not only to retrieve the army's honor and trust but also to preserve and protect our precious nature.

Figure 1.4: Officers from the ROK Marine 1st division explaining about their illegal wastewater discharge (Bae, 2014).

1.3 Phosphorus in Water

Phosphorus is an essential element that required by all living organisms such as plants and animals. It is used by these organisms for synthesizing cell structure and energy (e.g. Adenosine Triphosphate) (Paytan and Mclaughlin, 2007).

Among the anthropogenic sources of phosphorus such as plant fertilizers and human waste (e.g. sewage), agricultural effluent of overused fertilizer and livestock waste are a major phosphorus sources. Phosphorus contained in these sources is usually carried from lands to rivers and eventually transferred to lakes, and coastal waters. Finally, this essential element stimulates high growth of for aquatic autotrophic organisms such as algae and bacteria (Paytan and Mclaughlin, 2007). Eventually phosphorus brings about propagation of aquatic primary producers (e.g. algae) which require phosphorus for their growth. The rapid proliferation of organisms caused by excessive phosphorus is called eutrophication (Chislock et al., 2013).

Eutrophication in aquatic environments is potentially caused by both nitrogen and phosphorus. In freshwater systems, phosphorus is normally limiting, thus when excessive amounts of phosphorus are released from agricultural effluent and municipal sewage sources, it causes a drastic decrease in water quality (Lehtiniemi et al., 2005). Eutrophication results in algal bloom that alter aquatic ecosystems. The effects of eutrophication including eliminating species of fish and vegetation by decreasing light penetration that is caused by algal blooms (Chislock et al., 2013). The light is known for essential element to account for photosynthesis that produces oxygen (Eq.1). Following is an overall equation for the type of photosynthesis that occurs in normal plants in nature.

$$6CO_2 + 6H_2O + \text{sunlight} \rightarrow C_6H_{12}O_6 + 6O_2 \quad \text{(Eq. 1)}$$

Photosynthesis is important for aquatic organisms on account of producing oxygen. However, dead and decaying algae can cause insufficient oxygen (reverse of equation 1). Finally, this insufficient oxygen levels are toxic to fish and aquatic organisms. Thus eutrophication has been a serious environmental concern in much of the developed world for the past decades, and is now becoming a global concern (Jutidamrongphan, 2012).

Due to the negative effects of eutrophication, garrisons and camps located near Forward Edge of the Battle Area (FEBA) and DeMilitarized Zone (DMZ) have been suffering from water contamination (Research Institute for Kangwon, 2013). As a result, most of the small drainages for are polluted with green effluents. Following is a picture of eutrophication caused by excessive nutrients taken near the 3rd division at Kangwon province in northwestern of Republic of Korea in 2009. Eutrophication is already ongoing as it to be seen on the picture (Figure 1.5).

Figure 1.5: An example of contaminated small drainage by effluents near one garrison under command of 3rd division at Kangwon province (CWinews, 2009).

1.4 Phosphorus Speciation

Total phosphorus (TP) in wastewater consists of organic and inorganic species (Maher and Woo, 1998). Figure 1.5 represents the diverse phosphorus species that comprise TP. Total organic phosphorus (TOP) is made up of a diverseness of compounds including phosphonate, adenosine triphosphate (ATP), and organic phosphates (Maher and Woo, 1998). Inorganic phosphorus comprised of inorganic condensed phosphorus, polyphosphate, and orthophosphate (Maher and Woo, 1998).

Orthophosphate, which is known as reactive phosphorus (RP), presents in various forms and demonstrate a pH dependence of phosphorus. Figure 1.6 shows the relative amounts of phosphate in water with respect to wide range of pH (Parker et al., 2015).

Figure 1.7 shows that the most protonated species at low pH is H_3PO_4 and most deprotonated species at high pH is PO_4^{3-}. That is, dominant phosphate species change when pH increases or decreases.

The distribution diagram of phosphate was based on the following three equilibrium reactions.

$$H_3PO_4 \rightarrow H^+ + H_2PO_4^- \qquad K_a = 10^{-2.15} \qquad \text{(Eq.2)}$$

$$H_2PO_4^- \rightarrow H^+ + HPO_4^{2-} \qquad K_a = 10^{-7.20} \qquad \text{(Eq.3)}$$

$$HPO_4^{2-} \rightarrow H^+ + PO_4^{3-} \qquad K_a = 10^{-12.33} \qquad \text{(Eq.4)}$$

Based on Figure 1.7, specific pH range has different dominant phosphate species. For example, $H_2PO_4^-$ is the dominant orthophosphate species in the pH range of 2.2-7.2 whereas HPO_4^{2-} is the dominant orthophosphate species in the pH range of 7.2-12.3. Accordingly, phosphate species diagram can be an elucidation for pH dependence of phosphorus removal take advantage of an adsorption reaction. More about the adsorption reaction for phosphorus removal will be discussed and accounted for via surface complexation in section 1.6.

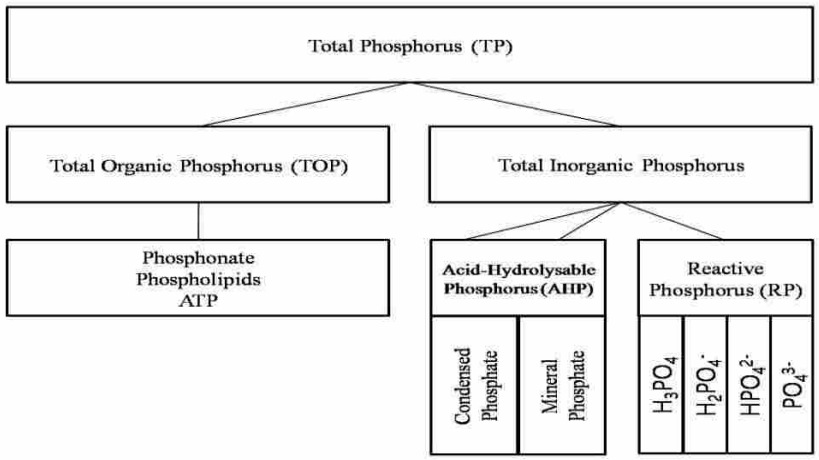

Figure 1.6: Classified Total Phosphorus Species in wastewater (Parker et al., 2015).

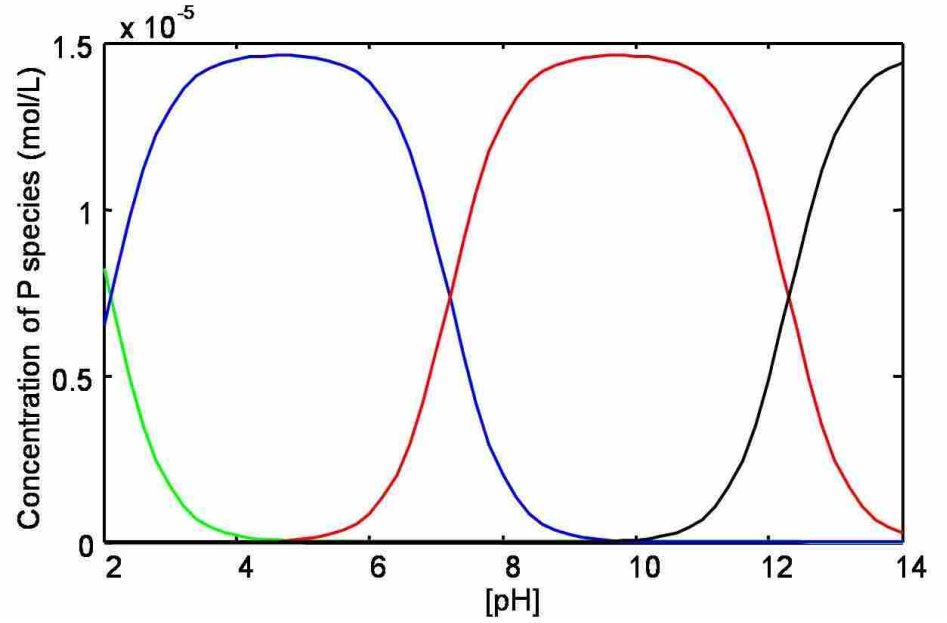

Figure 1.7: Distribution of orthophosphate over wide range of pH. Phosphoric acid (H_3PO_4) distribution is shown in green, $H_2PO_4^-$ is shown in blue, HPO_4^{2-} is shown in red and PO_4^{3-} is shown in black.

1.5 Phosphorus Removal Technologies

Phosphorus occurs in wastewater and surface water in inorganic forms (orthophosphate, polyphosphate) or organic forms such as phosphonate, ATP (Paytan and Mclaughlin, 2007). In wastewater treatment technologies, various techniques have been employed for phosphorus removal (e.g. adsorption, and membrane filtration process). Broad categories of phosphorus effluents treatment include physical, chemical and biological processes (Gray, 2012).

1.5.1 Physical Phosphorus Removal

Physical size of pollutants is generally used to account for physical phosphorus removal process (Gray, 2012). Specific processes are often used separately or in associated with other processes. One such process is sedimentation. By using the influence of gravity, this process makes particulate pollutants settle out of solution (Gray, 2012). The other process is filtration. Filtration is when a liquid is passed through a membrane or sand filtration and solids that cannot pass through the membrane are retained. The pore size of the filter (e.g. 2-50 nm for ultrafiltration, pore size < 2 nm for nanofiltration) or sand bed (e.g. effective size range of 0.45-0.65 mm for shallow-bed and 2-3 mm for deep-bed) directly influences the amount of solids which are retained in the filter (Gray, 2012; Metcalf and Eddy, 2003).

Reverse osmosis (RO) method is the tightest filtration method in wastewater treatment (Kim, 2003). RO separates solvent from dissolved solutes in solution by forcing the pressure that is higher than osmotic pressure through a semi-permeable membrane or filter (pore size < 2 nm). This process separates the water from dissolved contaminants in wastewater by utilizing pressure that is higher than the osmotic pressure (Kim, 2003). The small pores of membrane are restrictive to organic compounds such as pesticides. However, the primary limitation of RO is the high operating cost (Dialynas *et al*., 2008; P. H. Patton, 2013). A very high-quality feed is required for efficient operation of a RO unit and high trans-membrane pressure is also needed (Dialynas *et al*., 2008).

1.5.2 Chemical Phosphorus Removal

The chemically mediated phosphorus removal process is a well-known method for removing phosphorus. The process includes chemical coagulation, chemical oxidation processes, and chemical precipitation (Metcalf and Eddy, 2003; Jutidamrongphan, 2012). Chemical precipitation by the addition of the metal ions that form precipitates is well-known in wastewater treatment engineering. The most commonly used multivalent metal ions are Fe^{3+} and Al^{3+} (Metcalf and Eddy, 2003).

Treatment methods in which removal of pollutants is brought about by chemical reaction (e.g. chemical precipitation, chemical adsorption) are known as unit processes.

The unit operations and processes are gathered up to provide diverse levels of treatment, which are consist of preliminary, primary, secondary and tertiary (advanced) treatment. Finally, wastewater treatment process finish with disinfection (Gray, 2012; Hammer & Hammer, 2001; Metcalf and Eddy, 2003). To avoid maintenance or operational problems with the treatment operations or processes, preliminary treatment removes wastewater constituents such as rags, and floatables prior to the water entering primary treatment. During primary treatment, a portion of the suspended solids and organic matter from the preliminary treatment are removed. In secondary stages, remaining sludge such as biodegradable organic matter, suspended solids, and phosphorus are removed. Tertiary (or advanced) treatment is a comprehensive process following the primary and secondary process. This process removes residual suspended solids after secondary treatment. After these series of treatment, the wastewater moves through a disinfection stage. After completing this stage, effluent is released (Metcalf and Eddy, 2003). Figure 1.8 shows a generalized schematic flow chart for wastewater treatment processes explained above.

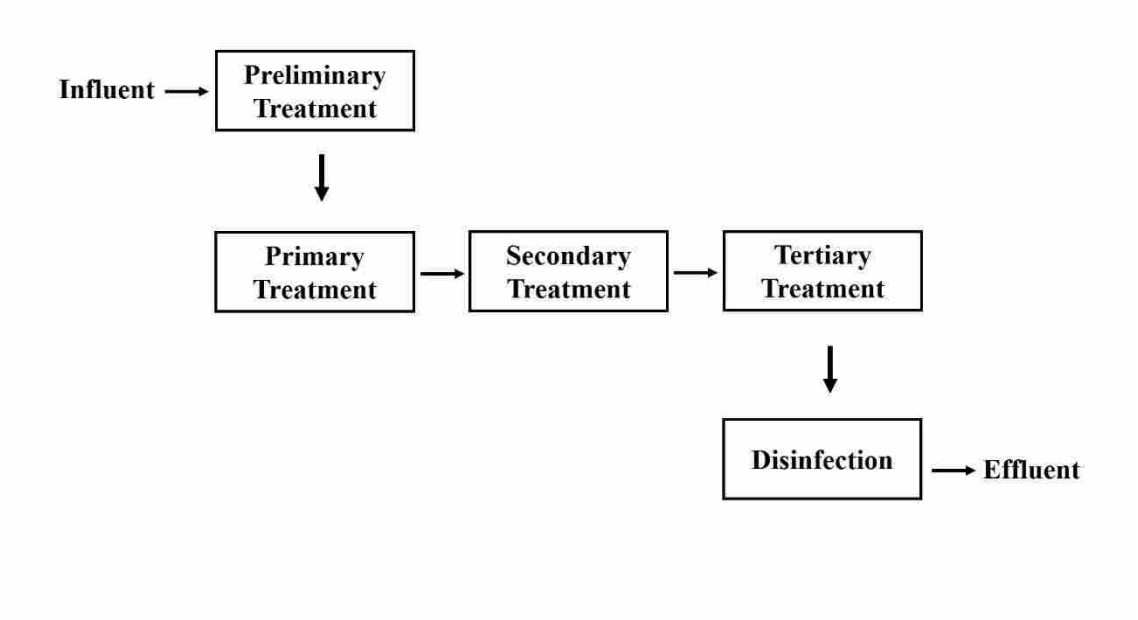

Figure 1.8: Basic flow chart schematic of wastewater treatment processes (Gray, 2012).

The metal salts typically used in the phosphorus removal process are $Ca(OH)_2$ (lime), $NaAlO_2$ (sodium aluminate) and $FeCl_3 \cdot 6H_2O$(ferric chloride) (Kim and Jeon, 2011). The addition of calcium or aluminum or iron salts to wastewater for phosphate removal result in the precipitation of $CaHPO_4$ (Calcium phosphate), $AlPO_4$ (Aluminum phosphate), and $FePO_4$ (Iron(Ⅲ) phosphate) respectively (Kim and Jeon, 2011). Once the chemical process is completed, the metal salt precipitates are removed in separate sedimentation facilities or with effluent filters (Metcalf and Eddy, 2003).

1.5.3 Biological Phosphorus Removal

The biological treatments of wastewater are to convert nutrients, such as

phosphorus and nitrogen into simple end product such as pure water. Generally, biological processes accelerate the growth of bacteria and encourage the bacteria hold large amounts of inorganic phosphorus in the so called biomass. Due to the greater specific gravity compare to water, the biomass can be removed by settling out of solution (Metcalf and Eddy, 2003). In biological phosphorus removal, phosphorus in poly-phosphates such as ATP, DNA (Deoxyribonucleic acid), and RNA (Ribonucleic acid) is accumulated in the sludge and removed by sedimentation. Certain microorganisms that bring about an achievement of this process are called polyphosphate accumulating organisms (PAOs). Under anaerobic conditions with fermentation products, PAOs release orthophosphate while taking advantage of the energy to accumulate simple organics and eventually store them as a form of polyhydroxyalkanoates (PHAs). Under aerobic conditions, the PAOs grow by using some of the energy to take up orthophosphate and store it as a form of polyphosphates. Enhanced biological phosphorus removal (EBPR) can remove phosphorus in the waste activated sludge. This can have around 5% or more phosphate (dry weight) whereas, non-EBPR sludge can have only 2-3% of phosphorus (Gray, 2012; Strom, 2006).

1.5.3.1 Ion Exchange

Ion exchange is a unit process in which ions of a given species are taken up in

place of an insoluble exchange material. This process in solution can be operated in two modes. First one is a batch mode. In a batch mode, the exchange resin is stirred in the treatment reactor until the reaction is complete. The spent resin is removed by settling and then regenerated and reused. The other mode is a continuous mode. In a continuous mode, the exchange resin is placed in a bed or a packed column, and waste water is passed through it (Metcalf and Eddy, 2003). Ion exchange has been effective for reducing and removing ionic contaminants (e.g. phosphorus) levels to low levels a range of 1μg/L to 1 g/L of contaminant concentration (Kentish and Stevens, 2001). However, due to some limitations such as necessity of the extensive pretreatment, considerations in terms of the life of the ion exchange resins and the complex regeneration system are required (Metcalf and Eddy, 2003).

1.6 Advanced Wastewater Treatment for Phosphorus Removal

Due to the necessity of removal of nutrients (e.g. phosphorus, nitrogen) beyond the abilities of conventional treatment processes, more advanced wastewater treatment is required. Consequently, increased engineering knowledge derived from studies and experiments for low level effluents are classified as advanced wastewater treatment methods (Metcalf and Eddy, 2003).

1.6.1 Adsorption for Phosphorus Removal in Wastewater Treatment

Adsorption is the process of accumulating an adsorbate that is in wastewater onto a sorbent surface. The accumulation of adsorbate takes place at the interface of adsorbent forming a two dimensional structure (Goldberg, 2013). The adsorbate is the material which is being removed from the adsorbent's interface (e.g. phosphate), while adsorbent is the solid, liquid, or gas phase for accumulation of adsorbate, such as activated carbon (Metcalf and Eddy, 2003). Usually, several transport steps are required for adsorption process. The first step is the movement of constituents from the bulk liquid to the boundary surface (Figure 1.9-1). At the boundary surface, there exists a stagnant liquid film. The stagnant liquid film is the layer that adsorbate have to penetrate by diffusion to enter pores of the adsorbent (Figure 1.9-2). Finally, the adsorption involves the attachment of the constituent to be adsorbed onto adsorbent's surface site (Figure 1.9-3) (Metcalf and Eddy, 2003; Parker et al., 2015). The adsorbate usually being described as a group of surface ligands while adsorption being considered as surface complexation (Benjamin, 2006).

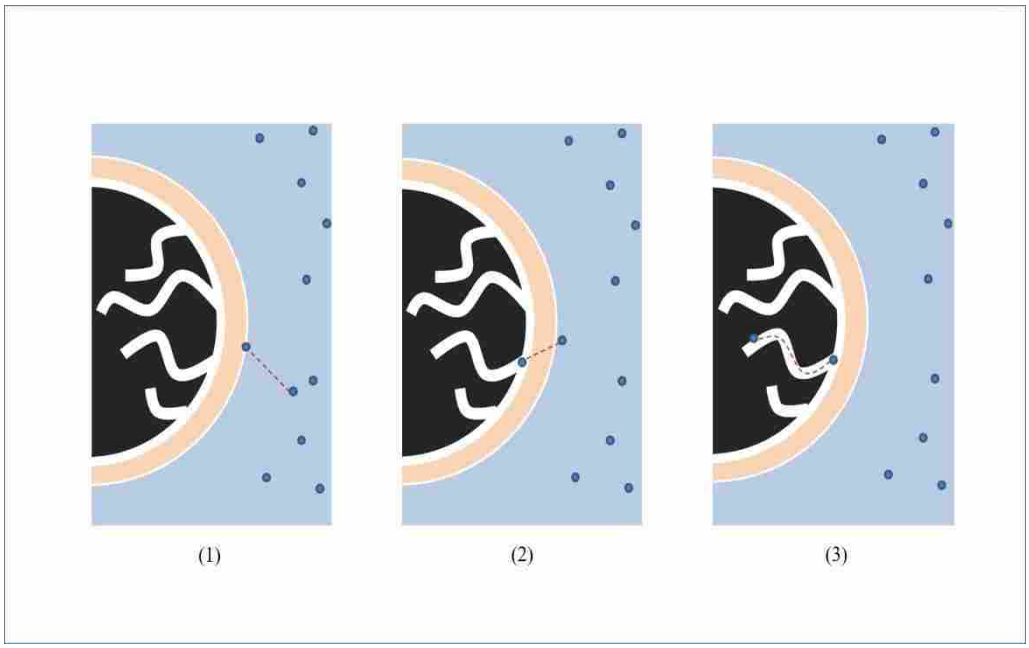

Figure 1.9: The adsorption process occurs in bulk solution. Blue circles represent adsorbate while black circles represent adsorbent (Parker et al., 2015).

1.6.1.1 Surface Complexation Model

The surface complexation model (SCM) was originally suggested by Stumm and Schinler to elucidate the adsorption between hydrogen ions or metal ions at the interface of oxide and water as a form of ion complexation (Shin, 1997). Basically, SCM is based on the complexation reaction between the functional group and the solid surface of the adsorbate, resulting in a coordinated bond. Theoretically, the fundamental concepts upon SCM are composed of following basic assumptions (Dzombak and Morel, 1990; Shin, 1997).

(1) Sorption onto metal oxides occurs at specific coordination sites.

(2) Sorption reactions onto metal oxides can be described by the law of mass

action.

(3) Surface charge and surface potential should be included in calculation of chemical reaction of surface group.

(4) Applied correction factor that origin from the electrical double layer theory to mass law constants for surface reactions can be taken into consideration for the effect of surface charge on sorption (Shin, 1997).

When surface of adsorbent is positively charged, anions can be adsorbed while forming inner and outer sphere surface complexes. This occurs in chemical wastewater removal when the phosphate ion sorbs on metal surfaces. Outer sphere complexes form from the interaction between ion pairs. Conversely, inner sphere complexes form through chemical bonding (i.e. covalent bonds) which can form a mono-dentate or bi-dentate complex (Zheng et al, 2012). For example, Figure 1.10 shows mono-dentate and bi-dentate inner sphere complexes. As denticity refers to how many times a single ligand coordinates to one acceptor, Figure 1.10 shows mono-dentate and bi-dentate complexes. In Figure 1.10, on the left side shows electron donor (oxygen ion) bound to metal surface, whereas on the right shows two electron donor groups to same metal surface.

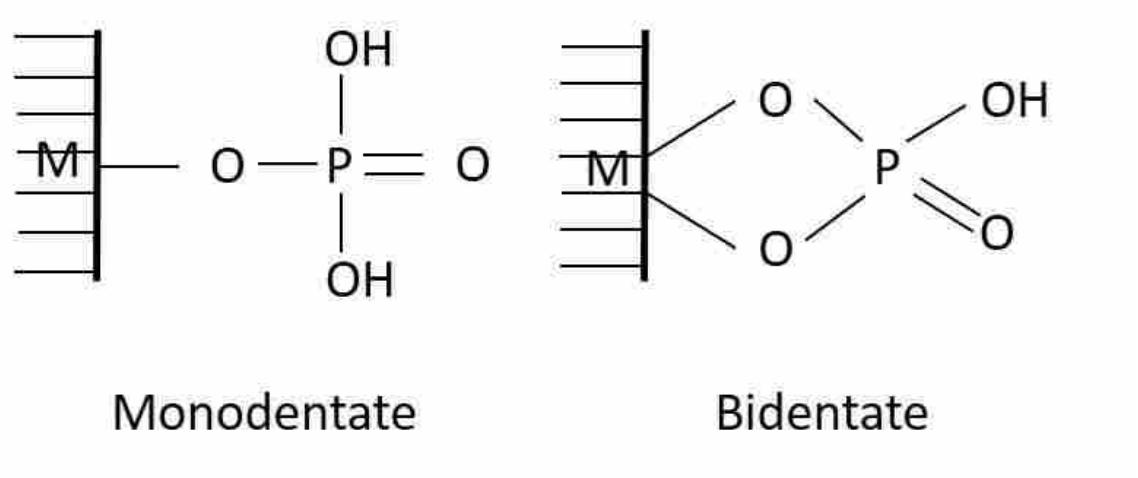

Figure 1.10: The complexes formed between phosphate and metal oxide. Slash lines represent the surface of metal oxide (adapted from Gray, 2012)

1.7 pH Dependence of Phosphate Removal in Wastewater Treatment

As a result of advances in simulation technology, wastewater treatment processes have been developed over the past 20 years (Metcalf and Eddy, 2003). For example, in chemical phosphorus removal, many parameters can be incorporated and used for optimal removal. Among these parameters (e.g. pH, time, dosage, and ionic strength) pH is one of the most important parameter for optimal removal of phosphorus (Tanada et al., 2003).

Especially in chemical removal, pH influences adsorption reactions as a result of proton competition for surface oxygen and phosphate oxygen which is based on surface complexation model mentioned in section 1.5.1.1 (Smith et al., 2008). In addition, due to electrostatic attractions between positively charged surfaces of adsorbents and phosphate ions, when initial pH is below the pH at the zero point of charge (pH_{ZPC}), it can be seen that maximum removal was obtained (Moharami and Jalali, 2014).

1.8 Research Goals and Objectives

The objectives of this research are summarized in the following list.

1. To characterize phosphorus species in a synthetic phosphorus solution and use colorimetry technique to measure residual phosphorus to calculate removal of phosphorus.
2. To relate phosphorus removal to adsorption reaction and determine how phosphorus can be removed via adsorption.
3. Simulating pH dependence of phosphorus removal through adsorption onto TiO_2.
4. Test with real and simulated wastewater the existing Photo-Cat system (Purifics, London) for phosphorus removal using TiO_2 nanoparticles, which may show more phosphorus removal due to its wide surface area compared to bulk powder.
5. Determine the optimal parameters for phosphorus removal process to enhance TiO_2 capabilities.

The first three objectives of this thesis will be addressed in Chapter 2: Determination of phosphorus adsorption onto TiO_2 bulk powder using colorimetry. In this chapter an auto colorimeter (AA3, Seal Analytical) and spectrophotometer are used to determine residual phosphorus in synthetic phosphorus samples.

Objectives four and five demonstrate the practical use of TiO_2 for phosphorus wastewater. The Photo-Cat (Ceramic Membrane System) will be discussed in Chapter 3:

Advanced wastewater treatment using Photo-Cat system with TiO_2 nanoparticles, which has been used for removing particles in wastewater. In Photo-Cat system, theoretically, by turning the UV lights on, oxidation step to convert non-reactive phosphorus (organics) to reactive phosphorus (orthophosphate) would occur. This may help phosphorus removal by surface complexation.

Supplementary information in terms of MATLAB code for modeling isotherm data can be found in the attached appendices.

1.9 References

Benjamin, M. M. (2006). Water Chemistry, 1st edition, McGraw Hill Korean Language edition, Seoul, Republic of Korea.

Chislock, M. F., Doster, E., Zitomer, R. A. & Wilson, A. E. (2013). Eutrophication: causes, consequences, and controls in aquatic ecosystems. *Nature Education Knowledge 4(4):10*. Retrieved from: http://www.nature.com/scitable/knowledge/library/eutrophication-causes-consequences-and-controls-in-aquatic-102364466

Choi, J. (2001). A study on operating control of wastewater treatment system in military. Master Thesis, Chosun University, Kwangju, Republic of Korea.

CWINews. (2009, March 25). Kangwon province, Improvement of water quality in cooperation with the army garrisons. Retrieved from: http://m.cwinews.co.kr/view.asp?intNum=2287&ASection=001001#

Dialynas, E., Mantzavinos, D., Diamadopoulos, E. (2008). Advanced treatment of the reverse osmosis concentrate produced during reclamation of municipal wastewater. Water Research, 42, 4603-4608.

Goldberg, S. (2013). Surface complexation modeling. *Earth systems and environmental sciences*, 1-14. Retrieved from: http://www.ars.usda.gov/sp2UserFiles/Place/20360500/pdf_pubs/P2433.pdf

Hammer, M. J. L., Hammer, M. J. J. (2001). Water and wastewater technology, 4th Edition. Prentice Hall, Upper Saddle River, New Jersey, USA.

Jutidamrongphan, W. (2012). Phosphorus removal from wastewater using selective adsorbents. Doctoral Thesis, Konkuk University, Seoul, Republic of Korea.

Gray, H. (2012). Laboratory methods for the advancement of wastewater treatment modeling. Master Thesis, Wilfrid Laurier University, Waterloo, ON, Canada.

Kentish, S. E., Stevens, G. W. (2001). Innovations in separations technology for the recycling and reuse of liquid waste streams. *Chemical Engineering Journal, vol. 84*, 149-159.

Kim, B. (2003). Application of mechellar-Enhanced ultrafiltration in the simultaneous removal of nitrate and phosphate. Master Thesis, Korea Advanced Institute of Science and Technology, Daejon, Republic of Korea.

Kim, J., Jeon, S. (2011). Treatment of phosphorus in sewage and wastewater. *Journal of the Korean Industrial and Engineering Chemistry*, vol. 14, No. 5, 12-21. Retrieved from: https://www.cheric.org/PDF/PIC/PC14/PC14-5-0012.pdf

Kim, S., Baumann, E, R. (1997). Investigation of chemical phosphate removal from an oxidation ditch by field evaluation. *Environment Engineering Research, Vol 2, No. 3*, 207-216. Retrieved from: http://www.eeer.org/upload/eer-2-3-207-7.pdf

Lehtiniemi, M., Engstrom-Ost, J., and Viitasalo, M. (2005). Turbidity Decreases anti-predator behavior in pike larvae, esox lucius. *Journal of Environmental Biology of Fishes, vol 73, Issue 1*, 1-8.

Maher, W., Woo, L. (1998). Procedures for the storage and digestion of natural waters for the determination of filterable reactive phosphorus, total filterable phosphorus and total phosphorus. *Analytica Chimica Acta*, 375, 5-47.

Metcalf and Eddy, Inc. (2003). Wastewater Engineering: Treatment and Reuse, 4th edition. McGraw Hill international edition, New York, USA.

Moharami, S., Jalali, M. (2014). Effect of TiO_2, Al_2O_3, and Fe_3O_4 nanoparticles on phosphorus removal from aqueous solution. *Environmental Progress & Sustainable Energy, Vol.33, No.4,* 1209-1219. doi:10.1002/ep.11917

Park. J. (2002). A study of reality of environmental pollution and solution plan in the military. Master Thesis, Kyounggi University, Seoul, Republic of Korea.

Parker, W., Gray, H. (2015). State of knowledge of the use of sorption technologies for nutrient recovery from municipal wastewaters, Water Environment Research Foundation, Vol.14. doi: 10.2166/9781780407319

Patton, P. (2013). Treatment of reverse osmosis brine with advanced oxidative processes for enhanced phosphorus removal. Master Thesis, Wilfrid Laurier University, Waterloo, ON, Canada.

Paytan, A., Mclaughlin, K. (2007). Phosphorus in our water, Oceanography, The Oceanography Society, vol. 20, No.2, 200-206. Retrieved from: https://pmc.ucsc.edu/~apaytan/publications/2007_Articles/Phosphate%20in%20our%20Waters.pdf

Research Institute for Kangwon. (2013). Rational enforcement of clean area total maximum daily load and the research of the cost of water quality preservation. Kangwon province, Republic of Korea. Retrieved from: http://www.prism.go.kr/homepage/entire/retrieveEntireDetail.do;jsessionid=361353E50FA40AEFD34790D7F0690EA2.node02?cond_research_name=&cond_research_start_date=&cond_research_end_date=&research_id=6420000-201300088&pageIndex=438&leftMenuLevel=160

Republic of Korea, Ministry of Environment. (2005). A study of reasonable improvement countermeasure of groundwater quality management and pollution remediation criteria. Retrieved from: http://www.waterindustry.co.kr/admin/bbs/down.php?code=data01&idx=5188&no=1

Republic of Korea, Ministry of Environment. (2011). Soil and groundwater contamination and surface water quality at military ground, Policy Report of Ministry of Environment. Article No.171-091-002. Retrieved from: http://webbook.me.go.kr/DLi-File/089/5510115.pdf

Republic of Korea, Ministry of National Defense. (2014). Defense white paper, Seoul, Republic of Korea. Retrieved from: http://www.mnd.go.kr/ user/mnd/upload/ pblictn/PBLICTNEBOOK_201506110235094860.pdf

Republic of Korea, National Institute of Environmental Research. (2000). Study on the water quality standard and criteria for the policy maker. Retreived from: http://theme.archives.go.kr/R/publication_ebook_2008/eBook_Contents/script_v1/open.jsp?BName=11148008300005301200007 08&BID=100029&PageNo=0&SID=5&BStyle=0&Title=%C1%A4%C3%A5%B0%E1%C1%A4%C0%DA%B8%A6+%C0%A7%C7%D1+%B0%A2%B1%B9%C0%C7+%BC%F6%C1%FA%B0%FC%B7%C3+%B1%E2%C1%D8+%BA%F1%B1%B3%BA%D0%BC%AE

Republic of Korea Army Head Quarter. (1999). Environmental preservation practical references. Field manual of Republic of Korea Army, Kyeryong, Republic of Korea. This article is prohibited to carry out of territory of the Republic of Korea.

Shin, Y. (1997). Research of adsorption modeling using surface complexation model. Master thesis, Keimyoung University, Daegu, Republic of Korea.

Smith, D. S., Takács, I., Murthy, S., Diagger, G., and Szabó, A. (2008), Phosphate complexation model and its implications for chemical phosphorus removal. *Water Environment Research* 80, 428–438.

Parker, W. & Smith, S., Gray, H. (2015). State of Knowledge of the Use of Sorption Technologies for Nutrient Recovery from Municipal Wastewaters, *Water Intelligence Online* **14**.

Strom. F. (2006). Technologies to remove phosphorus from wastewater, Retrieved from http://www.water.rutgers.edu/Projects/trading/p-trt-lit-rev-2a.pdf

Tanada, S., Kabayama, M., Kawasaki, N., Sakiyama, T., Nakamura, T., Araki, M., and Tamura, T. (2003). Removal of phosphate by aluminium oxide hydroxide. *Journal of Colloid and Interface Science 257,* 135-140.

Takács, I., Belia, E., Boltz, J. P., Comeau, Y., Dold, P., Jones, R., Morgenroth, E., Schraa, O., Shaw, A. and Wett, B. (2010). Structured Process Models for Nutrient Removal. In *Nutrient Removal: WEF Manual of Practice No. 34*; Water Environment Federation® (2010). WEF Press. Alexandria, VA.

The management and use of livestock excreta Act No. 12516, article No. 14. (2014). Retrieved from: https://elaw.klri.re.kr/kor_service/lawView.do?hseq= 32448&lang=ENG

Water quality and aquatic ecosystem conservation Act No. 12519, Article No. 26, attached No. 10 (2014). Retrieved from: https://elaw.klri.re.kr/ kor_service/ lawView.do?hseq=32485&lang=ENG

Zheng, T., Sun, Z., Yang, X., Holmgren, A. (2012). Sorption of phosphate onto mesoporous γ-alumina studied with in-situ ATR-FTIR spectroscopy. Chemistry Central Journal, 6:26, 1-10.

Chapter 2: Determination of phosphorus adsorption onto TiO_2 bulk powder using colorimetry

2.1 Introduction

There has been increasing demand for achieving low levels of total phosphorus (TP) due to more stringent water quality standards for effluent imposed on wastewater treatment plants (Liu *et al*., 2010). Thus, many wastewater treatment technologies for phosphorus removal have been used to attain low levels of phosphorus in wastewater (Gray, 2012). Subsequently, achieving low levels of TP that range from 0.1-0.3 mg P/L have been accomplished by modern technologies (Gu *et al*., 2007).

For detection of phosphorus concentration in wastewater, conventional phosphorus fractionation methods according to Standard methods (4500P-E) have been applied. The procedure based on the quantitative conversion of orthophosphates to a colored species, molybdenum blue, uses UV spectroscopy for measuring the absorbance of phosphorus and so called colorimetry methods (Gu *et al*., 2011). The colorimetric analysis is the most commonly used method, however, since phosphorus can be in water in various forms, a digestion step is needed for conversion of different forms of phosphorus to orthophosphate before using colorimetry methods (Smith, 2015). The digestion step is dependent on the fractions of phosphorus that are presented in Figure 2.1.

Both total reactive P (tRP) and soluble reactive P (sRP) do not need any digestion

steps because forms of P in tRP and sRP can be measured by colorimetric analysis without further digestion (Maher and Woo, 1998; Patton, 2013). For total P (TP), an ammonium persulfate digestion method is used to measure phosphorus in samples (Smith, 2015). By this method, various forms of phosphorus can be converted into orthophosphate. An acid hydrolysable digestion (tAHP) is used for total acid hydrolysable P (tAHP) and soluble acid hydrolysable P (sAHP) (Patton, 2013).

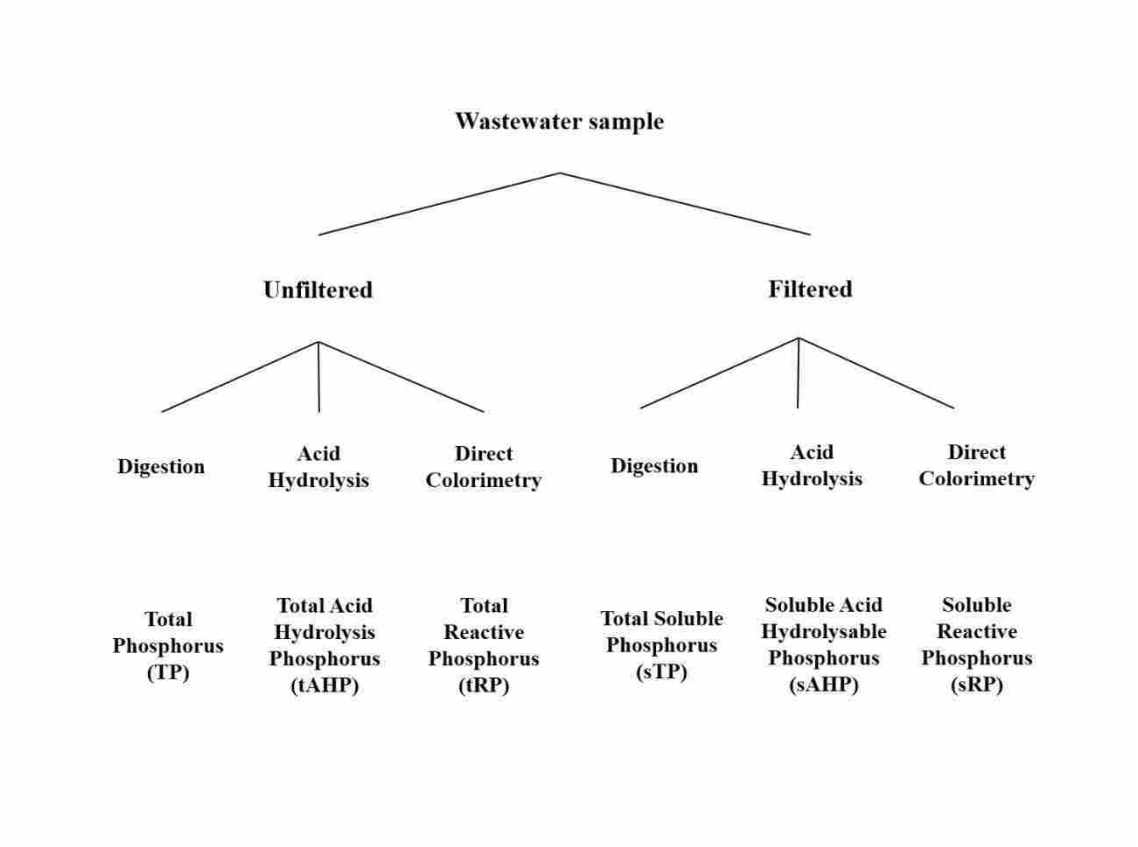

Figure 2.1: Analytical methods for determining diverse fractions of phosphorus (Gray, 2012). Filtered species can pass through 0.45μm filter.

In this chapter, soluble reactive P (sRP) will be measured by colorimetry via ascorbic acid method for calculating the amount of removed phosphorus by TiO_2 bulk powder.

Colorimetry methods will be discussed in section 2.2 below.

2.2 Colorimetric Analysis of Phosphorus

For detection of phosphorus in samples, the ascorbic acid method, which is the most common method, was used (Doolittle, 2014). In the ascorbic acid method, steps shown in Figure 2.2 are carried out to measure color.

The first step shown in Figure 2.2 is adding sulfuric acid (H_2SO_4) for acidification of the sample to convert phosphate to phosphoric acid. Important to note if pH is too low, molybdenum species can form in the sample that do not react with phosphate (Smith, 2015).

After forming the phosphoric acid (H_3PO_4), potassium antimonyl tartrate ($K_2(Sb)_2(C_4H_2O_6)$) and ammonium-molybdate ($(NH_4)_6Mo_7O_{24}\cdot 4H_2O$) are added (shown in Figure 2.2) so that phosphomolybdic acid ($H_3PMo_{12}O_{40}$) can form. In this step, the role of antimonyl salts is to accelerate the color forming reaction (Smith, 2015). The next step is reducing the phosphomolybdic acid using ascorbic acid to yield reduced molybdenum blue complex. During this reduction reaction, ascorbic acid gives two electrons to the complex, therefore, reducing it (Doolittle, 2014; Smith, 2015). Ascorbic acid as a reducing agent has a significant advantage since it is less sensitive to salts during the reaction. Of course, the ascorbic acid method also has a shortcoming, which is the slow

colour development time. However, this problem can be fixed by adding potassium antimonyl tartrate (explained above). After forming molybdenum blue complex, the absorbance can be measured by spectrophotometer. Generally, absorbance is measured at wavelengths of 660 or 880 nm depending on required sensitivity (Smith, 2015).

The final step is color development (shown in Figure 2.2 as time) which is related to time and subsequent measuring of the color in Figure 2.3. Despite wide variation of literature recommendations (i.e. less than 10 minutes from Drummond and Maher, (1995); 10 to 30 minutes from Eaton *et al*., 2005), recommended method of auto analyzer were used. This experimental procedure followed empirical data based on the results by Smith, 2015.

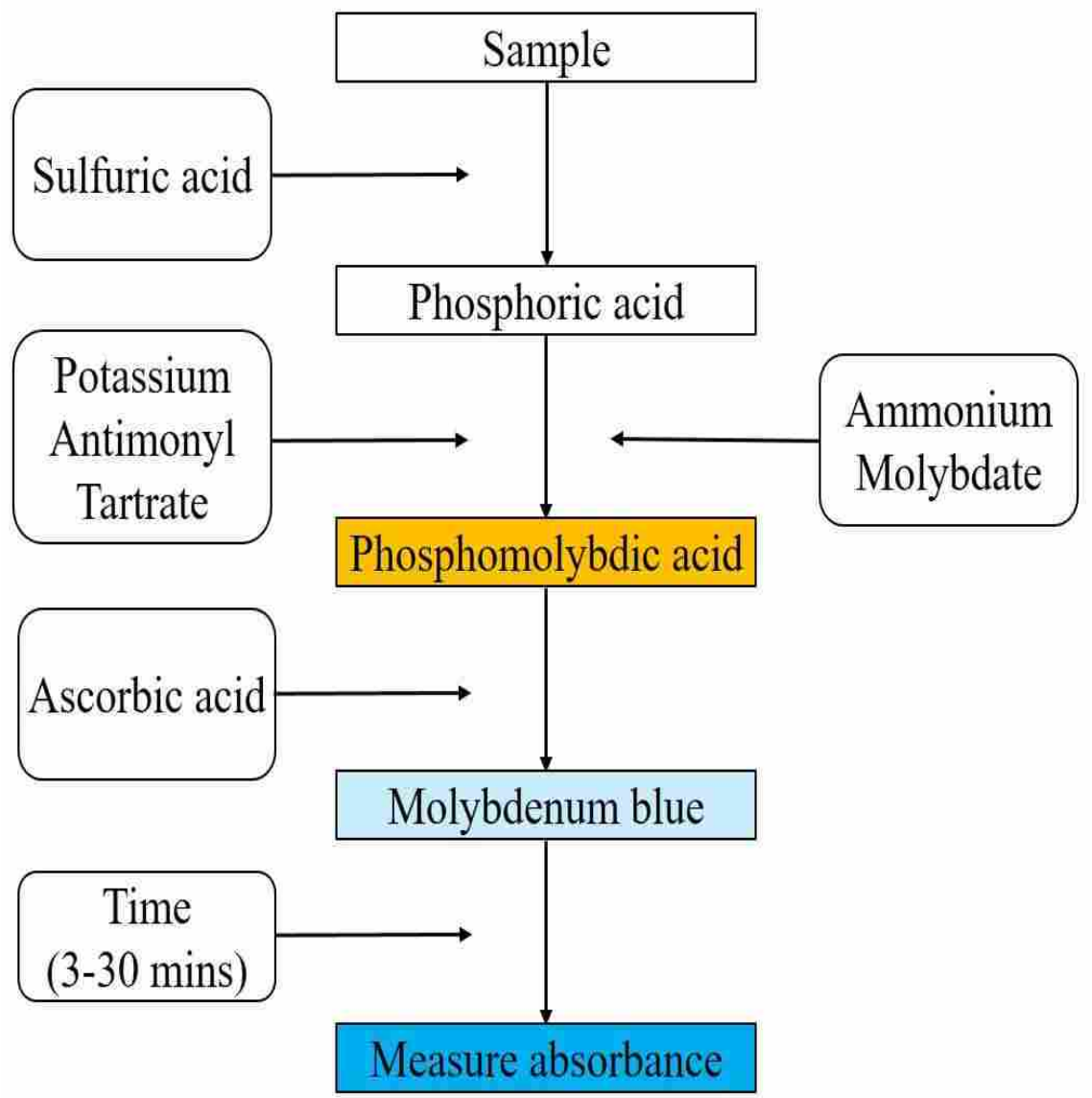

Figure 2.2: Schematic diagram of overall steps of colorimetric analysis. The yellow colored box shows phosphomolybdic acid and the light blue box represents the reduced phosphomolybdic acid complex (Smith, 2015).

Figure 2.3 demonstrates that 3 to 30 minutes of color development time is reasonable for phosphorus determination using spectrophotometer (SM 4500P-E) (Smith, 2015). In Figure 2.3, if color development time is too little (time < 3 minutes) or too long

(time > 30 minutes), a systematic underestimation of concentration will result. Thus, if the systematic error tolerance is 10%, shown in Figure 2.3 as dashed line, 3 to 30 minutes represent reasonable time of color development for phosphorus determination using spectrophotometer (SM-4500P-E). The data shown in Figure 2.3 overlaps with recommended in Standard Methods recommended in Eaton *et al*, 2005.

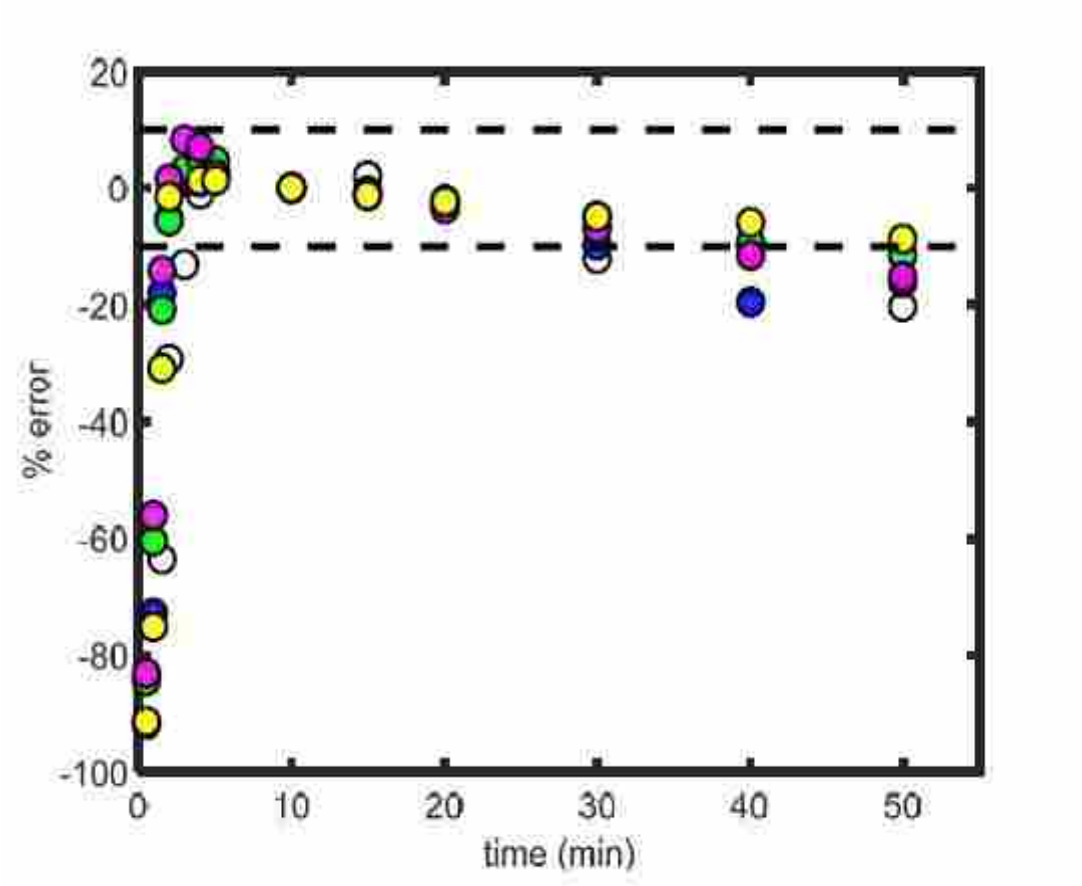

Figure 2.3: Absorbance versus time for phosphorus solutions. Dashed lines represent ±10% systematic error. Based on this data, a period of 3 to 30 minutes for time development has been recommended in previous research and this recommendation is similar to prior research (Eaton et al, 2005; Smith, 2008). (Smith, 2015).

The colorimetric method, based on the Beer-Lambert's law, can measure concentration of orthophosphate using spectrophotometer (Harris, 2002). During the experiments, instead of spectrophotometer, auto colorimeter (auto analyzer) was used for rapid and accurate experiment. Auto colorimeter also following the Beer-Lambert's law for measuring concentration of orthophosphate. According to the Beer-Lambert's law Shown in equation (2.1), concentration (*c*) of orthophosphate is proportional to the measured absorbance (*A*) of a colored complex (Harris, 2002).

$$A = \varepsilon lc \qquad \text{(Eq.2.1)}$$

In the equation, ε is the molar absorptivity, l is the path length (cm) and c is the concentration of absorbing species in moles per liter (mole/L). Duplicate samples were measured using a 1 cm path length quartz cuvette at 660 nm or 880 nm. Light intensity was also measured, and absorbance was calculated based on the equation 2.2.

$$A = - \log (P/P_0) \qquad \text{(Eq.2.2)}$$

Where, *A* is absorbance, *P* is the light intensity measured from the sample, and P_0 is the light intensity measured from the blank standard. Based on this data, a calibration curve was plotted. Concentrations of each sample were calculated using the equation of the linear line fit into the calibration standards. The graph below is an example of a calibration curve (Figure 2.4). In this graph, the range of phosphorus was 0.1-0.8 mg

P/L and the correlation coefficient was 0.980 which demonstrates the accuracy of this linear line.

Based on Figure 2.4, we know the linear line in the diagram is y=0.545x+0.015. In this equation, y represents absorbance and x represents phosphorus concentration.

Thus unknown phosphorus concentration of samples can be calculated by substituting for the y value. In short, by transforming the Eq.2.1, x can be described as

$$x = \frac{(y-0.015)}{0.545} \qquad \text{(Eq.2.3)}$$

As absorbance *A* (*y* in Eq.2.3) was measured for unknown phosphorus concentration in the experiments, the parameter x (represents *c* in Eq 2.1) value is easily calculated.

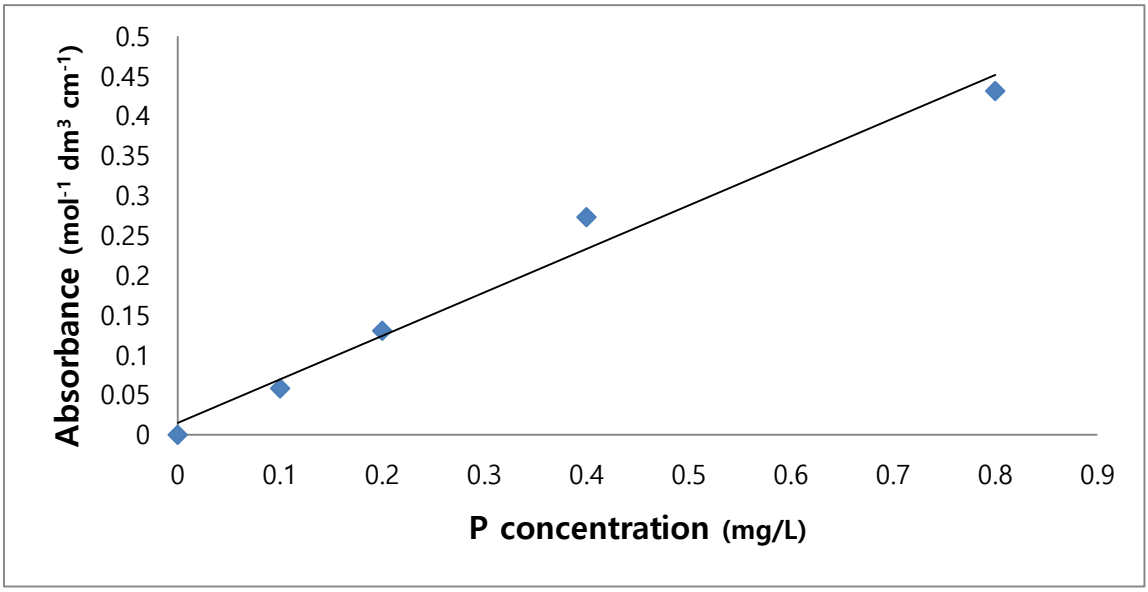

Figure 2.4: An example calibration curve plotted using measured data. The range of concentration of phosphorus samples was 0.1mg-0.8mg P/L. The equation of the linear line in the graph is A=0.545c+0.015, R2=0.980.

2.3 Methodology

2.3.1 Sample Preparation

All the solutions used in the experiments were prepared from certified reagent grade chemicals, which were used without any further purification. Reaction vessels were treated with 5% HNO_3 and rinsed 2-times with Milli-Q water before they were used.

Calibration standards were prepared from 1000 mg P/L stock solution made using KH_2PO_4. Standard concentrations ranged between 0.25 - 7 mg P/L. Blanks (0.0 mg P/L) were prepared using Milli-Q water. All samples and calibration standards were measured in duplicate.

For the pH dependence experiment, phosphorus samples were prepared by diluting the stock solution of 1000 mg P/L that prepared by dissolving KH_2PO_4 in Milli-Q water to 2 mg P/L. Sample pH range were varied from 4 to 10 using 0.1M HCl or 0.1M NaOH while maintaining an ionic strength of 0.1 to 0.01M KNO_3. The dosage of TiO_2 was fixed at 400 ± 40 mg/L weighed using weigh balance (Mettler Toledo, Mississauga, ON, Canada).

For the adsorption isotherm experiment, phosphorus samples were prepared using the same stock solution as above, with a range of 0.1 to 100 mg P/L while sustaining an ionic strength of 0.01M KNO_3. A sample pH and TiO_2 dosage were fixed at 400 ± 40 mg/L , respectively.

Each sample replicate was measured using auto colorimeter (SEAL Analytical, Kitchener, ON, Canada), that is automated spectrophotometer, which allows for a faster and more accurate sample measurement. Auto colorimeter produces corrected absorbance that are calculated based on calibration standards plotted by itself. The data was analyzed using Excel for conversion of unit (i.e. mol/L) which was used in previous literature (Moharami and Jalali, 2014; Tanada et al, 2003). MATLAB^{TM} (MathWorks, Natick, MA, USA) was used to fit experimental data to isotherm models and visualize the data.

2.3.2 Reagents and Materials

2.3.2.1 pH dependence and adsorption isotherms

Mixed reagent recipe and the color development method were applied from Standard Methods for Examination of Water and Wastewater (1998). An auto colorimeter (SEAL Analytical, Kitchener, ON, Canada) was used for determining phosphorus concentration by ascorbic acid method. The mixed reagent was prepared in combination with sulfuric acid (H_2SO_4) (98+%, EMD Millipore, USA), ascorbic acid (98+%, Alfa Aesar, USA), ammonium molybdate ($H_{24}Mo_7N_6O_{24}\cdot 4H_2O$, Sigma Aldrich, USA) and potassium antimonyl tartrate ($C_8H_4K_2O_{12}Sb_2\cdot 3H_2O$, 99+%, Sigma Aldrich, USA). For preparing 50 mL volume of mixed reagent, 25 mL 5N H_2SO_4 added to 2.5 mL of potassium antimonyl tartrate and 7.5 mL ammonium molybdate. Then the solution was

diluted to 50 mL with 15 mL of 0.1M ascorbic acid.

For synthesizing the sample, monopotassium phosphate (KH_2PO_4, 99%, VWR, USA) was added to Milli-Q water (18.2MΩ, Milli-Q water) and a sample of 2 mg P/L was made, while maintaining an ionic strength of 0.01M KNO_3 (99.9%, Sigma Aldrich, USA). The samples were mixed using a rocker (VWR, USA) for 24 hours. After that, samples were filtered by 0.45μm membrane filter (VWR, USA). Lastly, the auto analyzer was used to measure absorbance for samples.

There were subtle differences between pH dependence and adsorption isotherms experiments. In case of pH dependence, concentration of phosphorus has to be fixed to measure optimal pH for phosphorus removal using TiO_2 bulk. However, as adsorption isotherm is the process to find equilibrium phosphorus concentration, phosphorus concentration of sample varies (range of 0.05 mg-10 mg P/L) while pH is fixed at 4.0. For TiO_2 bulk powder, three types of TiO_2 were used and are rutile (99.9%, Sigma Aldrich, USA), anatase (99.8%, Sigma Aldrich, USA) and mixed powder (99.9%, Sigma Aldrich, Japan). They were used to determine pH dependence to select the most efficient TiO_2 type while mixed powder is used during the adsorption isotherm experiment.

2.4 Result and Discussion

The adsorption of phosphorus onto TiO_2 bulk powder was measured by the auto

colorimeter. Each time measurements were made, all samples were prepared daily. Figure 2.5 shows examples of the daily calibration standard curve that were plotted. In Figure 2.5, the x axis represents phosphorus concentration in sample (mg/L) and the y axis represents peak height in digital units (%, percentile scale).

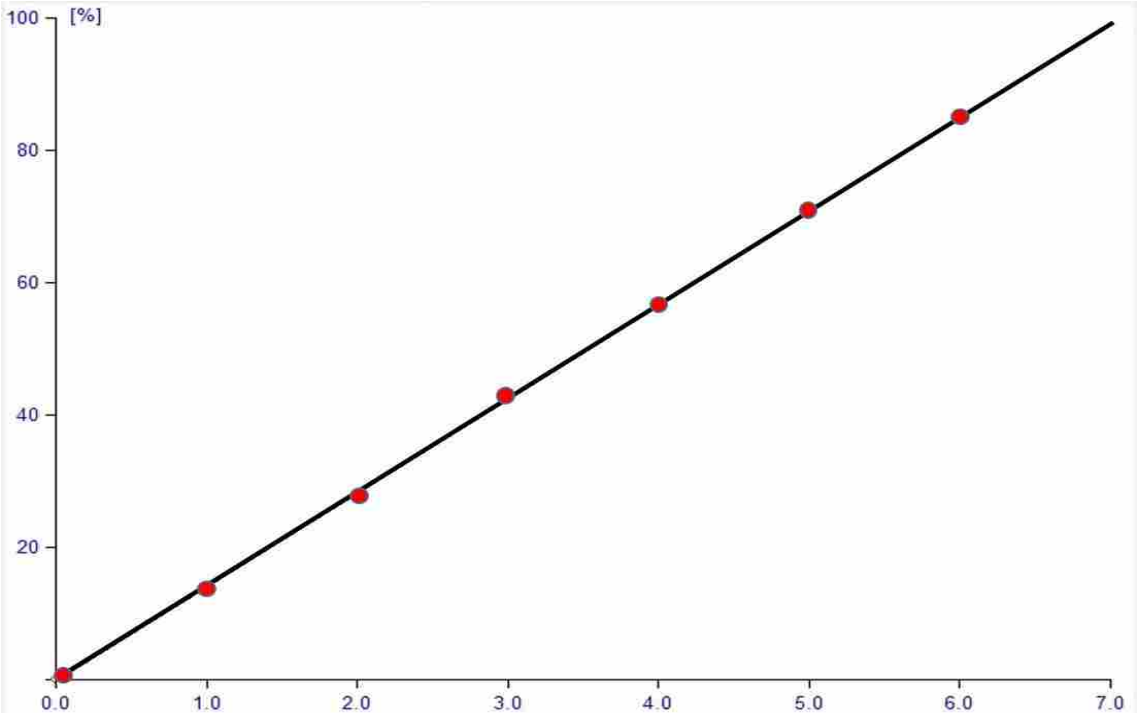

Figure 2.5: Examples of the calibration curve. In this graph, the x axis represents phosphorus concentration (mg/L), the y axis represents peak height in digital unit (auto analyzer converts absorbance to peak height in digital unit). Red dots represent measured samples.

The equations for calculation of phosphorus concentration in auto analyzer is summarized in Table 2.1. The correlation between the y axis and the x axis is sustained. Auto analyzer convert measured absorbance to peak height in digital unit. Thus actual absorbance value is not shown in this graph.

Table 2.1: The equation of Figure 2.5 for estimating correlation coefficient of calibration curve. In this table, *x* represents peak height in digital units (%) and y represents concentration of standards.

Correlation coefficient ($R^{2)}$	Calibration curve Equation
0.9999	$y = 4.99 \times 10^{-5}x - 1.56 \times 10^{-1}$

2.4.1 pH Dependence of Phosphorus Removal using TiO_2 Bulk Powder

The adsorption of phosphorus onto TiO_2 bulk powder was measured over a wide range of phosphorus concentrations at a fixed ionic strength of 0.01M KNO_3 at pH 4 to 10. A pH value is a significant parameter which can affect the adsorption process at the water-metal surface interfaces (Moharami and Jalali, 2014). Determining pH dependence of phosphorus adsorption on TiO_2 bulk powder and finding the optimal pH for adsorption is the first step to understand actual phosphorus removal (Moharami and Jalali, 2014).

Removed phosphorus by rutile, anatase, and commercially mixed (rutile + anatase) TiO_2 bulk powder decreases when pH increases (Figure 2.6). Interestingly, specific pH dependence patterns in terms of phosphorus interactions with other metal oxides such as aluminum has been reported. (Connor and Mcquillan, 1999; Tanada et al., 2003; Smith et al., 2008; Kang et al., 2011; Moharami and Jalali, 2014; Smith and Gray, 2014). For example, according to Smith and Holly, 2014, the phosphorus adsorption onto aluminum oxides shows 'U' shape in terms of pH dependence shown in

Figure 2.7. It can be observed that optimal phosphorus removal occurs around pH 6.

TiO_2 exists in nature as three different types of crystal form, which are known for rutile, anatase, and brookite. In terms of characteristics, both anatase and rutile have tetragonal structure and rutile is thermally stable. Anatase is converted into rutile when it is heated above 900℃.

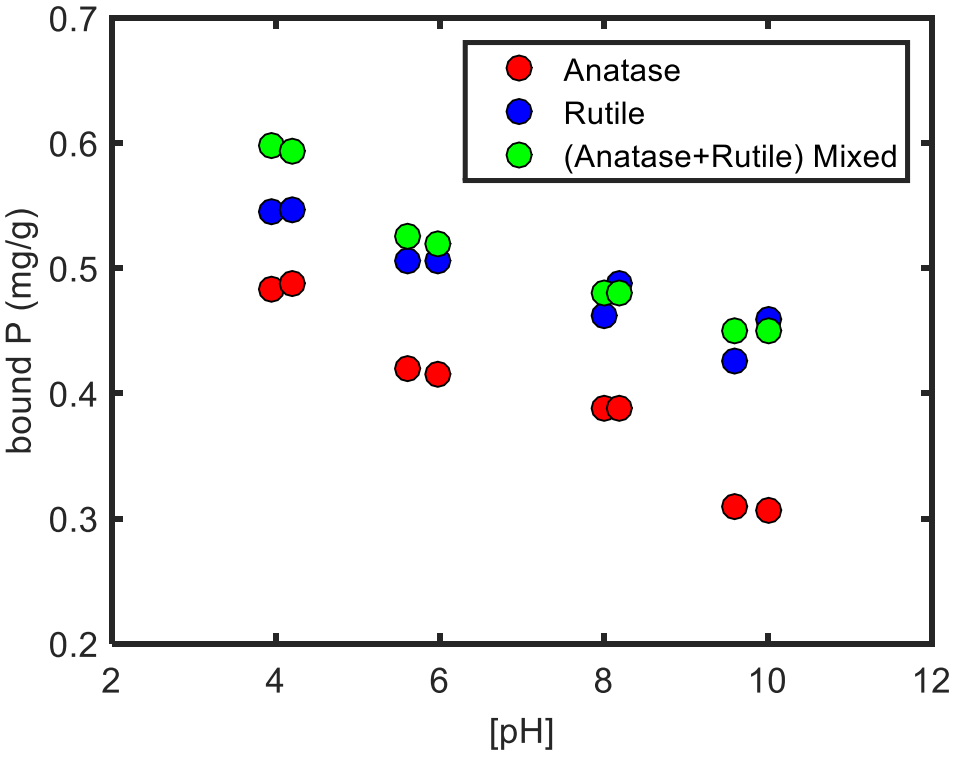

Figure 2.6: Three types of TiO_2 bulk powder show maximum phosphorus removal at around pH 4. The green dots achieved the highest efficiency of phosphorus adsorption onto TiO_2. It is shown that maximum bound phosphorus was achieved when using mixed TiO_2.

Although aluminum oxides also have pH dependence when they react with phosphorus, the trends, optimal pH and adsorption efficiency are different from TiO_2

(Smith and Gray, 2014; Moharami and Jalali, 2014). Thus, these distinctions can bring about different usage of metal species in practical fields (e.g. wastewater treatment).

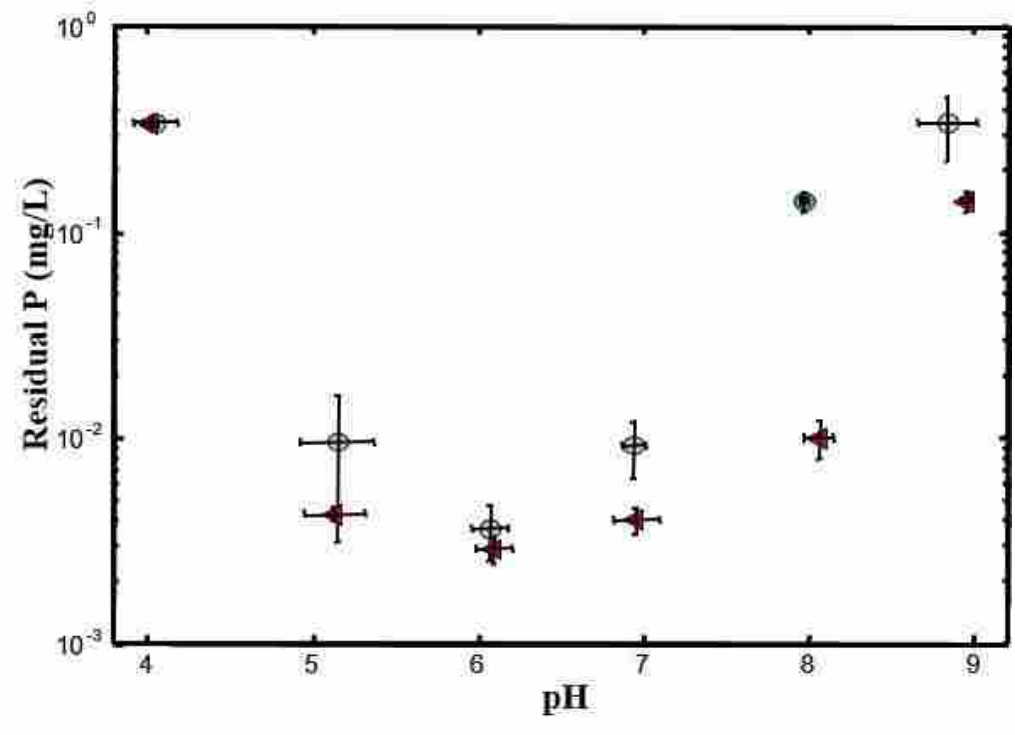

Figure 2.7: Phosphorus removal with both dosage of 5 mg Al/L (blue dots) and 10 mg Al/L (red trianges) with 1 mg P/L. Both dosage show 'U' shape in terms of pH dependence (Smith and Gray, 2014).

As it is shown in Figure 2.6, when pH decreases, adsorbed phosphorus increases. According to Figure 2.8, as pH changes, the dominant phosphorus species in a sample also changes. Thus, Figure 2.8 can be a possible explanation for pH dependence (Kang et al., 2011). For example, at around pH 4 to 7, $H_2PO_4^-$ was the dominant species, whereas at around pH 7 to 10, HPO_4^{2-} was the dominant species. Thus, these different types of phosphorus species can influence adsorption reactions onto TiO_2 bulk powder surface.

pH dependence of phosphorus adsorption can be explained by the function of pH (Kang et al., 2011; Moharami and Jalali., 2014).

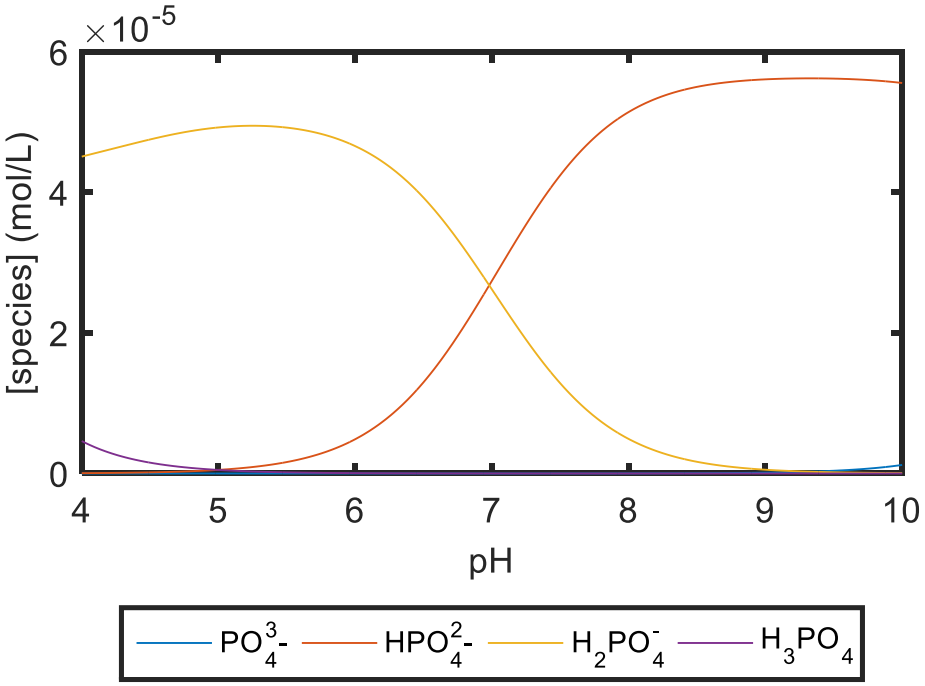

Figure 2.8: Phosphorus speciation diagram of concentration of 2mg P/L (6.4*10-5 mol/L) plotted by MATLAB™. The pH value varied 4 to 10 during the experiment.

In addition, the surface charge of TiO_2 bulk powder can be another demonstration of pH dependence. In Figure 2.9, it can be seen that at a range of pH 4 to 10, there are three differently charged titanium oxide species, TiO^-, TiOH, and $TiOH_2^+$. As the proton state at the titanium oxide surface changes, so too does the surface charges. For example, above pH 6.3 the concentration of the negatively charged species TiO^- is more than that of $TiOH_2^+$ species which means surface of titanium may be charged negatively (Kang et

al., 2011). This Figure 2.9 may be accounted for by pH point of zero charge theory below.

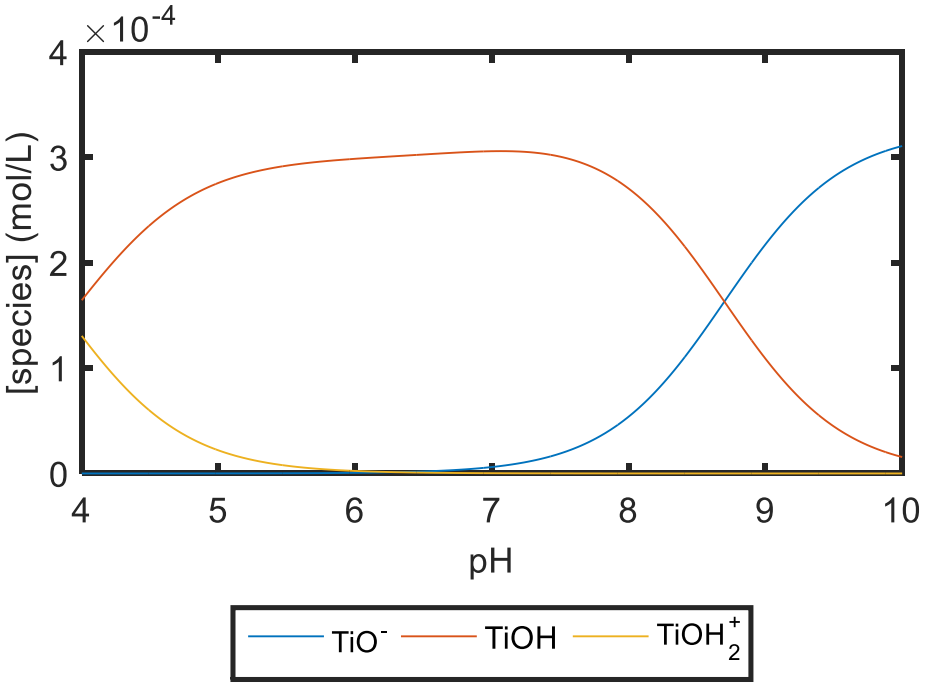

Figure 2.9: TiO_2 species of concentration of 400 ± 40 mg/L. The surface charge condition can account for pH dependence of orthophosphate.

Based on the charge state mentioned above, at around pH 6.3, it is shown that the titanium oxide surface charges 'zero'. Basically, the y axis of Figure 2.9 represents species concentration of titanium oxide. However, due to neutral surface of TiOH species, both TiO^- and $TiOH_2^+$ can affect surface charge state (Tombacz, 2009). Thus, at around pH 6.3 where the yellow line and the blue line intersect in Figure 2.9, titanium oxide surface has a net neutral charge. Theoretically, this unique pH value is known as pH point of zero charge (pH_{PZC}) (Kosmulski, 2002). Thus, the point zero of charge, described as

$[\equiv TiOH_2^+] = [\equiv TiO^-]$ (i.e. symbol of '≡' represents surface sites on TiO_2) is attributed to the reaction between titanium oxide surface and water molecules to form hydroxyl groups on oxide surface for completing its coordination sphere (Tombacz, 2009).

Experimentally measured pH_{PZC} can be calculated according to equation 2.4 (Tombacz *et al*., 2000; Tombacz, 2001). Thermodynamic equilibrium constants (log K) for solving equation 2.4 to determine theoretic pH value is in the Table 2.2.

$$pH_{PZC} = 0.5(\text{Log } K^{int}{}_{a,1} - \text{Log } K^{int}{}_{a,2}) \quad \text{(Eq.2.4)}$$

Table 2.2: Thermodynamic equilibrium constant for equation 2.5 (adapted from Stone *et al*., 1993).

Surface complexation reactions	Log K
$\equiv SOH + H^+ \leftrightarrow \equiv SOH_2^+$	3.9
$\equiv SOH + H_2O \leftrightarrow \equiv SO^- + H^+$	-8.7

Based on the equilibrium constants given in the Table 2.2, theoretical pH_{PZC} value can be simply calculated (Eq.2.5).

$$pH_{PZC} = 0.5[3.9 - (-8.7)] \quad \text{(Eq.2.5-1)}$$

$$pH_{PZC} = 0.5(3.9 + 8.7) \quad \text{(Eq.2.5-2)}$$

$$\therefore pH_{PZC} = 6.3 \quad \text{(Eq.2.5-3)}$$

The calculated pH_{PZC} of 6.3 (E.q.2.5-3) is in accordance with not only the value

from this experimental data but also previous research papers in terms of pH_{PZC} (Stone *et al*., 1993; Preocanin and Kallay, 2005; Tombacz, 2009; Moharami and Jalali, 2014). The pH_{PZC} based on Figure 2.9 does not mean the actual point of zero charge, which can be determined by calculation of net proton surface excess (Tombacz, 2009). Although there is no net proton surface excess data, Figure 2.9 coincides with surface electroneutrality point based on the mass titration method (Preocanin and Kallay, 2005). In addition, actual pH_{PZC} reported in Tombacz, 2009 was 6.23, which is very close to the pH_{PZC} calculated above. Thus, it seems that surface charge state as shown in Figure 2.9 may be used for determination of pH_{PZC}.

When the pH is above point of zero charge, the surface charge becomes more negative. However, if pH is below point of zero charge, the charge state of surface charge becomes positive. All three TiO_2 species show maximum amount of phosphorus removal when sample's pH is below 6.3. Thus, the amount of adsorbed phosphorus is higher due to titanium oxide surface that is charged positively (e.g. $TiOH_2^+$). Because electrostatic attraction takes place between $TiOH_2^+$ and phosphate ions and this has to be taken into account with regard to adsorption.

For modeling the experimental data, the surface complexation model (SCM) for hydrous ferric oxide (HFO) is used as referred from previous research (Smith *et al*.,

2008).

According to Smith *et al*. (2008), the SCM calculation is run to determine how much phosphate is bound to the iron oxide's surface (e.g. HFO) and other available oxygen binding sites. If the stoichiometry of the surface reactions can be determined, those possible reactions are taken as reasonable reactions that are possible on the iron oxide, and the sites that binding occurs are the active phosphate binding sites.

To quantify a value for soluble phosphorus which is not bound to iron oxide surface, total binding site capacity was used in tableau notation referred to as S1T and S2T. These two binding sites are considered to have the same value.

Based on SCM, in the tableau notation presented in Table 2.3, the total binding site capacity for TiO_2 surfaces are referred to as S1 and S2. Table 2.3 represents the chemical equilibrium modeling process based on Tableau notation (Morel and Herring, 1993). This modeling considers the TiOH, PO_4^{3-}, and H^+ as a set of simultaneous equilibria, including H^+ and PO_4^{3-} binding. The components that are located in the top of the Table are given, and the products made from these components are listed as species in the Table. The Tableau notation in Table 2.3 is plotted by MATLAB™.

The log K values for titanium species in Table 2.3 were obtained to describe the actual experimental data. It is considered that these two binding sites have the same

value. This can be related to the total titanium concentration (Ti_T) in the sample (Smith et al., 2008; Smith and Gray, 2014;).

$$S1 = S2 = ASF * (Ti_T) \text{ (Smith et al., 2008)} \quad \text{(Eq.2.6)}$$

Where, the ASF (Actual Site Factor) is the essential parameter in surface complexation model and Ti_T is total Ti species concentration. In this research, ASF value of 1.3 was used, which means 1.3 phosphate ions can bound to a single titanium atom (Smith and Ferris, 2001; Smith et al., 2008).

Based on the experimental data, the best fit value of log K for titanium species ($TiOPO_3^{2.5-}$, $TiO_2PO_2^{2-}$, and $TiOPOOH^-$) are 14.3, 25.1, and 29.6, respectively. The log K values that are obtained by fitting are shown in Table 2.3 marked as '※'. This best fit model calculation is shown in Figure 2.10 below. However, although this modeling could be used to predict phosphorus removal onto TiO_2 bulk powder but more data is necessary for complete validation.

Table 2.3: Tableau notation for chemical equilibrium system. The log K value for the last three species measured and calculated in this experiment were fitted by surface complexation model (Smith et al., 2008). S1 and S2 in the top column represent binding site of surface. On S1, surface oxygen is shared with 2 titanium atoms whereas, on S2, surface oxygen is bound to only 1 titanium atom. Last three log K value for titanium species were determined by fitting the experimental data from this research.

H^+	S1	PO_4^{3-}	S2	species	Log K
1	0	0	0	H^+	0
0	1	0	1	TiOH	0
0	0	1	0	PO_4^{3-}	0
0	0	0	0	S2	0
-1	0	0	0	OH	-14
1	1	0	0	$TiOH_2^+$	3.9
-1	1	0	0	TiO-	-8.7
1	0	1	0	HPO_4^{2-}	11.66
2	0	1	0	$H_2PO_4^-$	18.64
3	0	1	0	H_3PO_4	20.65
1	0	1	1	$TiOPO_3^{2.5-}$	14.3※
2	1	1	0	$TiO_2PO_2^{2-}$	25.1※
3	1	1	0	$TiOPOOH^-$	29.6※

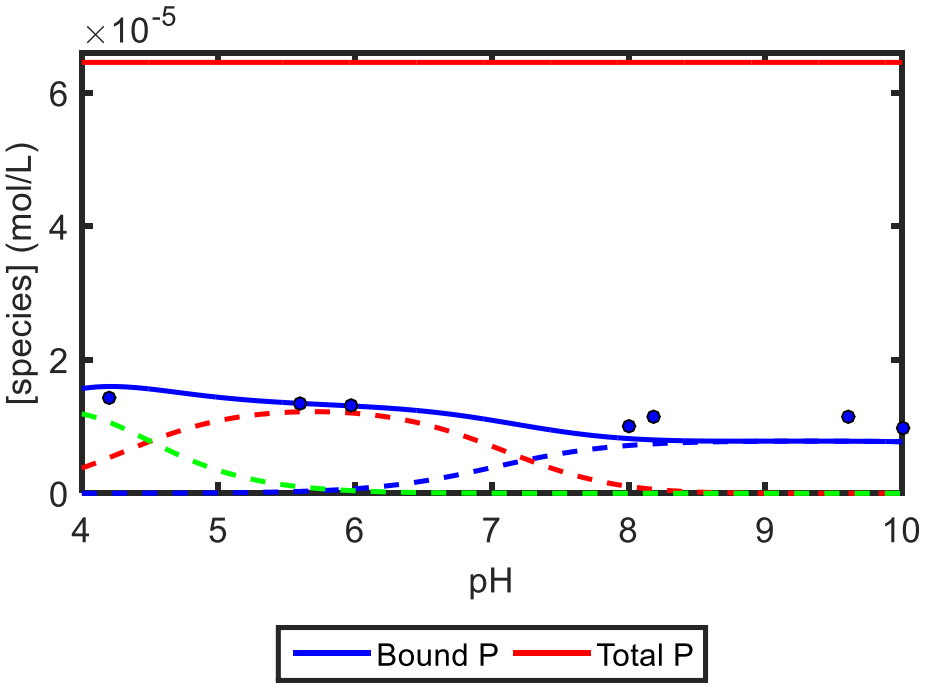

Figure 2.10: Bound phosphorus concentration from initial concentration of 2mg P/L (6.54*10-5 M). Collected data is represented as blue dots and the model calculation for ASF is 1.3 (shown as a blue solid line) while the solid red line represents initial P concentration. The three dashed lines demonstrate the trend of phosphorus removal. Dashed lines represent $TiO_2PO_2^{2-}$ (red), $TiPO_3^{2.5-}$ (blue), and TiO_2POOH- (green), respectively. The maximum removal of P was about 27% at pH 4.

2.4.2 Isotherms of Phosphorus Adsorption onto TiO_2 Bulk Powder

The equilibrium isotherms for phosphorus adsorption by TiO_2 bulk powder were performed at pH 4.5±0.5 which is considered optimal pH for adsorption as shown in section 2.4.1. The adsorption was measured by adding 0.25 to 10mg/L of phosphorus at fixed ionic strength of 0.01M KNO_3 electrolyte and the amount of TiO_2 bulk powder (mixed) used was 400 ± 40 mg/L. The amount of adsorbed phosphorus onto TiO_2 bulk

powder was calculated using equation 2.6 by fitting the experimental data to both Langmuir and Freundlich model through MATLAB™.

The Langmuir and Freundlich isotherm models are described as equation 2.7, and equation 2.8, respectively, below.

$$X = \frac{C*LT*KL}{C*KL+1} \quad \text{(Eq.2.7)}$$

Where, X is the amount of adsorbed phosphorus on solid phase (mg/L), C is equilibrium phosphorus concentration in solution phase (mg/L), L_T is maximum binding capacity (mg/L), and K_L is equilibrium adsorption constant (L/mg), which related to affinity of binding site.

$$X = K_F * C^{1/n} \quad \text{(Eq.2.8)}$$

Where, X is the amount of adsorbed phosphorus on solid phase (mg/L), C is the equilibrium phosphorus concentration (mg/L), K_F represents the Freundlich isotherm constant (mg/g), and n is the adsorption intensity (Dada, A.O *et al*., 2012).

The adsorption trend of phosphorus onto TiO_2 bulk powder is shown in Figure 2.10. The adsorbed phosphorus onto TiO_2 bulk powder increases drastically at first, and then, reaches a plateau and only increases slightly. That is, at low phosphorus concentrations, greater proportion of phosphorus can be adsorbed. This type of adsorption trends has been reported in previous papers (Kang et al., 2011; Moharami and Jalali,

2014).

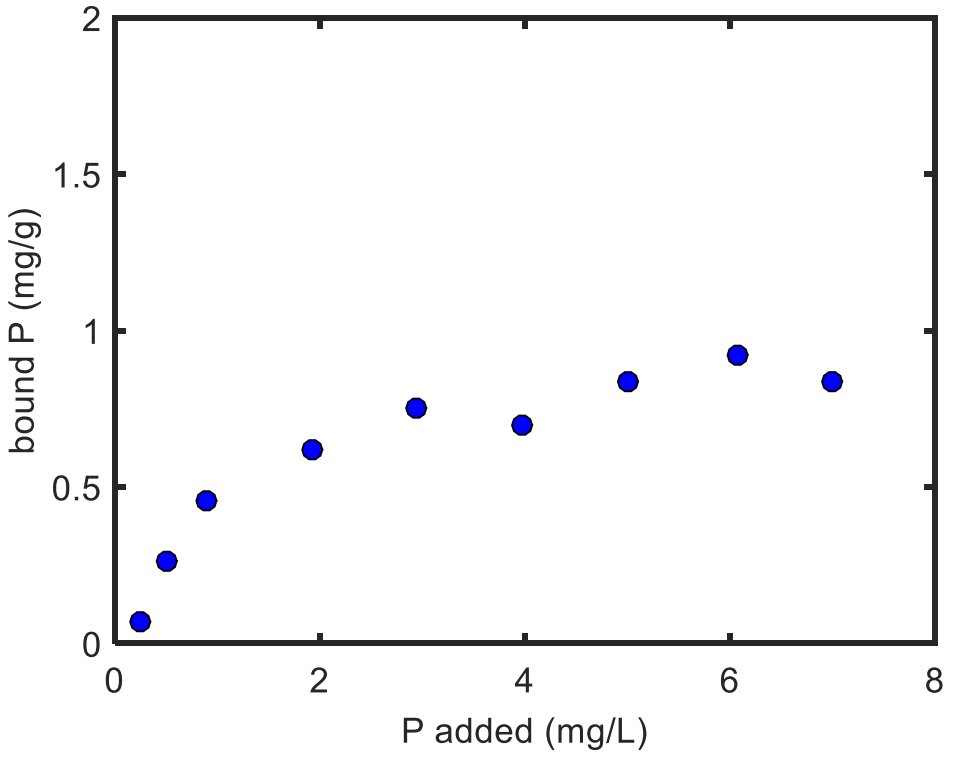

Figure 2.10: Phosphorus adsorption onto mixed TiO_2 bulk powder over a range of phosphorus concentration at 0.01M (KNO_3) ionic strength. The adsorption of phosphorus seems to reach a plateau and shows slight increasing above 2mg/L of phosphorus concentration.

Figure 2.11 which is shown below, was plotted to determine the maximum binding capacity of phosphorus on TiO_2 bulk powder. Figure 2.11 shows a plot of the adsorbed phosphorus by TiO_2 against the phosphate equilibrium concentration in the solution. Both the Langmuir and Freundlich equations that were explained above were used to describe the adsorption isotherm. The equilibrium constant and binding capacity for both models are shown in Table 2.4. As mentioned above, Figure 2.10 shows that

phosphorus adsorption data seem to reach plateau above 2 mg P/L. The equilibrium distribution of metal ions between solid and liquid phase can be explained by Langmuir model, the best fit model should be Langmuir model (Dada *et al*, 2012).

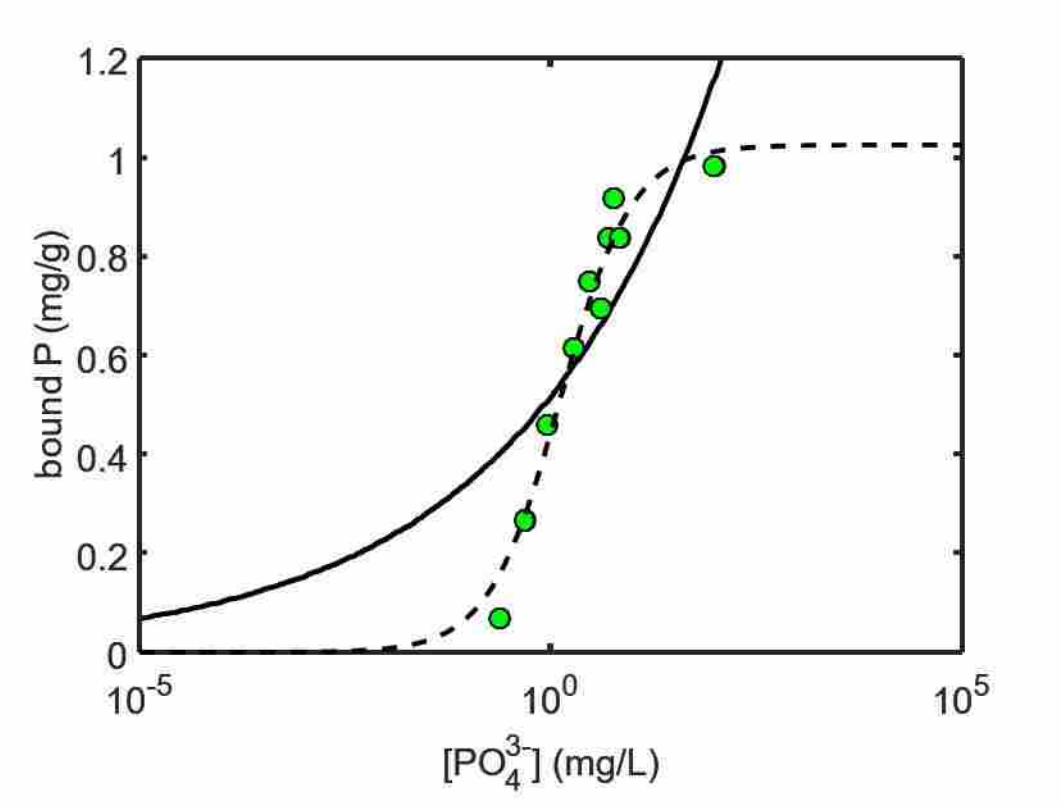

Figure 2.11: Both Langmuir (dashed line) and Freudlich (solid line) isotherm of phosphorus adsorption by TiO_2 bulk powder at pH 4.0 ± 0.2. Green dots represent actual experimental data in terms of bound phosphorus on adsorbent. It is shown that green dots better fit into the Langmuir model.

2.5 Conclusion

The phosphate removal by TiO_2 bulk powder (anatase, rutile, and mixed species) was investigated to determine pH dependence and adsorption trends. Due to surface area of bulk powder, less phosphates were adsorbed onto titanium species compared to

previous literature, that used TiO_2 nanoparticles in their experiments (Kang et al., 2012; Moharami and Jalali, 2014). However, bulk powder did show pH dependence and a maximum uptake of phosphate was measured at around 20% of initial phosphorus concentration onto mixed TiO_2 bulk powder. The pH was adjusted from 4 to 10 and it is shown that at around pH 4, optimal phosphate removal was achieved.

As pH changes during the experiments, dominant phosphate species also change. In other words, the function of pH can influence phosphorus adsorption. Thus, this may be an explanation for pH dependence. Another explanation is pH point of zero charge. It is shown that there are three types of titanium species (i.e. TiO^-, TiOH, and $TiOH_2^+$) during the adsorption experiments. The proton state at the titanium oxides' surface may affect adsorption. At around pH 6.3 which is the base point of charge state and also called point of zero charge, surface charge becomes zero. If pH goes down below 6.3, surface charges positively; if it is higher than 6.3, surface charges negatively. Consequently, affinity to bind on the surface of phosphate may be influenced by zero point of charge.

The isotherm trends were studied based on two different models which are the Langmuir and Freundlich models to determine binding capacity, adsorption intensity (n) and log K value. The binding capacity and log K value for Langmuir model was 0.77mg/g and 1.03L/mg, respectively, and heterogeneity factor and log K value for the Freundlich

model was 5.67 and 0.52mg/g, respectively.

Based on this experimental data, TiO_2 could show certain amount of phosphorus removal. However, it seems that more experimental results using TiO_2 will be needed to compared to other metal oxides such as aluminum or iron oxide for determination of the removal efficiency.

2.6 References

Connor, A. P., McQuillan, J. A. (1999). Phosphate Adsorption onto TiO_2 from Aqueous Solutions: An in Situ Internal Reflection Infrared Spectroscopic Study. *American Chemistry Society(ACS), Langmuir, 15(8),* doi:10.1021/la980894p, 2916-2921.

Dada. A. O., Olalekan. A. P., Olatunya. A. M., Dada. O. (2012). Langmuir, Freundlich, Temkin and Dubinin-Radushkevich isotherms studies of equilibrium sorption of Zn^{2+} unto phosphoric acid modified rice husk. IOSR Journal of Applied Chemistry Vol. 3, Issue. 1, 38-45

Doolittle, P. (2014). Ascorbic acid method for phosphorus determination, Retrieved from: http://community.asdlib.org/activelearningmaterials/files/2014/06/Lake_Study_Ascorbic_Acid_Method_for_Determining_Phosphorous.pdf

Drummond, L., Maher, W. (1995). Determine of phosphorus in aqueous solutions via formation the formation of the phosphoantimonylmolybdenum blue complex: re-examination of optimum conditions for the analysis of phosphate. *Analytica Chimica Acta, 302(1),* 69-74

Eaton, A. D., Clesceri, L. S., Rice, E. W., Greenberg, A. (2005). Standard methods for the examination of water and wastewater. American Public Health Association (APHA), American Water Works Association (AWWA) & Water Environment Federation (WEF), Washington, DC, USA, 21st edition

Gray, H. (2012). Laboratory methods for the advancement of wastewater treatment modeling. Master Thesis, Wilfrid Laurier University, Waterloo, ON, Canada.

Gu, A.Z., Neethling, J.B., Benisch, M., Clark, D., Fisher, D., Fredrickson, H.S. (2007). Advanced Phosphorus Removal from Membrane Filtrate and Filter Filtrate Using Packed Columns with Different Adsorptive Media. Proceedings of the Water Environment Federation, WEFTEC 2007: Session 91 – 100. San Diego, CA, 7899-7914.

Gu, A.Z., Majed, N., Benisch, M., Neethling, J. (2009). Fractionation and Treatability Assessment of Phosphorus in Wastewater Effluents-Implication on Meeting Stringent Limits. Proceedings of the Water Environment Federation, WEFTEC 2009. Orlando, FL, 804-806.

Harris, C. Daniel. (2002). Quantitative Chemical Analysis, 5th edition. W.H. Freeman and Company Korean Language edition, Seoul, Republic of Korea.

Kang, S. A., Li, W., Lee, H. E., Phillips, B. L., Lee, Y. J. (2011). Phosphate Uptake by TiO2: Batch studies and NMR spectroscopic Evidence for Multisite Adsorption. *Journal of Colloid and Interface Science, Vol. 364(2)*, 455-458.

Kosmulski, M. (2002). The pH-Dependent Surface Charging and the Point of Zero Charge. *Journal of Colloid Interface Science, Vol. 253, Issue 1*, 77-87.

Liu, L., Neethling, J. B., Stensel, H. D., Murthy, S., Gu, A. Z. (2012). Treatability and Fate of Various Phosphorus Fractions in Different Wastewater Treatment Processes. Water Science Technology 2011:(4):804-10. Doi: 10.2166/wst.2011.312

Maher, W., Woo, L. (1998). Procedures for the storage and digestion of natural waters for the determination of filterable reactive phosphorus, total filterable phosphorus and total phosphorus. *Analytica Chimica Acta, 375*, 22-33.

Moharami, S., Jalali, M. (2014). Effect of TiO_2, Al_2O_3, and Fe_3O_4 nanoparticles on phosphorus removal from aqueous solution. *Environmental Progress & Sustainable Energy, Vol.33, No.4*, 1214-1215.

Morel, F. M. M., Hering, J. G. (1993). Principles and Applications of Aquatic Chemistry. John Wiley and Sons, New York, USA

Patton, P. (2013). Treatment of reverse osmosis brine with advanced oxidative processes

for enhanced phosphorus removal. Master Thesis, Wilfrid Laurier University, Waterloo, ON, Canada, 37-39.

Preocanin, T., Kallay, N. (2006). Point of Zero Charge and Surface Charge Density of TiO_2 in Aqueous Electrolyte Solution as Obtained by Potentiometric Mass Titration. *Croatia Chemistry Acta, 79(1),* 100-104.

Parker, W. & Smith, S, Gray, H. (2015). State of Knowledge of the Use of Sorption Technologies for Nutrient Recovery from Municipal Wastewaters, *Water Intelligence Online* **14**.

Smith, S. (2015). Phosphorus analysis in wastewater: best practices, International Water Association, VOL. 15, 2016, doi:2166/9781780407807.

Smith, D. S., Takács, I., Murthy, S., Diagger, G., and Szabó, A. (2008). Phosphate complexation model and its implications for chemical phosphorus removal. *Water Environment Research* 80, 428–438.

Smith, S., Gray, H. (2014). Surface Complexation Modeling and Aluminum Mediated Phosphorus. Water Environment Federation, Nutrient Recovery and Management 2011, 970-977.

Smith, D. S., Ferris, F. G. (2001). Proton Binding by Hydrous Ferric Oxide and Aluminum Oxide Surfaces Interpreted Using Fully Optimized Continuous pK_a Spectra. Environment Science Technology, Vol 35(23), 4637-4641.

Standard Methods for the Examination of Water and Wastewater. (1998). American Public Health Association (APHA) and American Water Works Association (AWWA) and Water Environment Federation (WEF), Washington D.C., USA.

Stone, A., T., Torrents, A., Smolen, J., Vasudevan, D., Hadley, J. (1993). Adsorption of Organic Compounds Possessing Ligand Donor Groups at the Oxide/Water Interface. Environment Science Technology, 27(5), 895-909.

Tanada, S., Kabayama, M., Kawasaki, N., Sakiyama, T., Nakamura, T., Araki, M., and Tamura, T. (2003). Removal of phosphate by aluminum oxide hydroxide, *Journal of Colloid and Interface Science, Vol. 257*, 138-140.

Tombacz, E. (2009). pH-dependent Surface Charging of Metal Oxides, *Chemical Engineering 53/2*, doi:10.3311/pp.ch.2009-2.08, 80-84.

Tombacz, E., Szekeres, M., Klumpp, E. (2001). Interfacial Acid-Base Reactions of Aluminum Oxide Dispersed in Aqueous Electrolyte Solutions. 2. Colorimetric Study on Ionization of Surface Sites. *American Chemistry Society(ACS), Langmuir, 17(5)* doi:10.1021/la001323b, 1422-1425.

Zhang, G., Liu, H., Liu, R., Qu, J. (2009). Removal of Phosphate from water by a Fe-Mn binary Oxide Adsorbent. *Journal of Colloid and Interface Science 335*, 168-173.

Chapter 3: Advanced Wastewater Treatment using Photo-Cat system with TiO_2 nanoparticles

3.1 Introduction

In the 18th century, the Industrial Revolution occurred in Europe which contributed to changes affecting many aspects of human life (i.e. mass production). After the Industrial Revolution, there have been drastic increases in global population and economic growth (Lim, 2013). However, these developments potentially bring about severe destruction of nature which may cause serious environmental pollution (Choi, 2013). Thus, environment protecting technologies have been developed for several decades in order to help ensure environmental sustainability (Hashimoto et al., 2005; Lim, 2013).

Photocatalysis is one of the environmentally sustainable technologies. Photocatalysis is a catalytic process which takes place on the surface of semiconducting materials such as TiO_2 under ultra violet (UV) light irradiation (Noh, 2003; Lim, 2013). In fact, TiO_2 powders have been used as white pigments for a long time due to their chemically stable state, nontoxicity to humans, and cost efficiency in industrial fields (Hashimoto *et al*., 2005). In early 1970's, two Japanese researchers named Fujishima and Honda found that when TiO_2 is irradiated by UV light, TiO_2 can split water to hydrogen and oxygen (Fujishima and Honda, 1972; Choi, 2013).

TiO_2 Photocatalysis has been applied to various fields (i.e. environmental protection, renewable clean energy production). Typically, TiO_2 Photocatalysis is used for air purification (i.e. removal of air pollutants) and water purification (i.e. removal of dangerous substances) (Lim, 2013). Nowadays, technology using Photocatalysis is considered to be one of the most promising technologies for its potential to be applied to environment field friendly (Lim, 2013).

Photocatalysis is defined as acceleration of a photoreaction in the presence of a catalyst when light is irradiated (Yang, 2006). Thus, when TiO_2 absorbs light as a photocatalyst with greater energy than its band gap energy, a pair of electron holes (photogenerated charge carriers) are produced. These electron holes are separate and subsequently move from the bulk to the surface of the TiO_2 (Lim, 2013). Adsorbed water molecules react with separated electrons and form hydroxyl radicals (●OH) while separated holes form superoxide radicals ($O_2●^-$) by reacting with oxygen in the atmosphere. The reduction and oxidation reactions can be caused by both hydroxyl radicals and superoxide radicals (Lim, 2013). Figure 3.1 shows schematics of Photocatalysis which can occur when UV light irradiates TiO_2. Both superoxide radicals and hydroxyl radicals can participate in reduction or oxidation reactions to degrade contaminants from a wastewater sample. Hydroxyl radicals which have an especially

outstanding oxidation ability, can potentially break down organic pollutants such as VOCs (Volatile organic compounds), wastewater, and other industrial waste (Lim, 2013). Thus, using TiO_2 might convert organic phosphorus to phosphate which is removed by methods such as chemical phosphorus removal. Because organic phosphorus usually can not be removed by conventional methods described in Chapter 1.

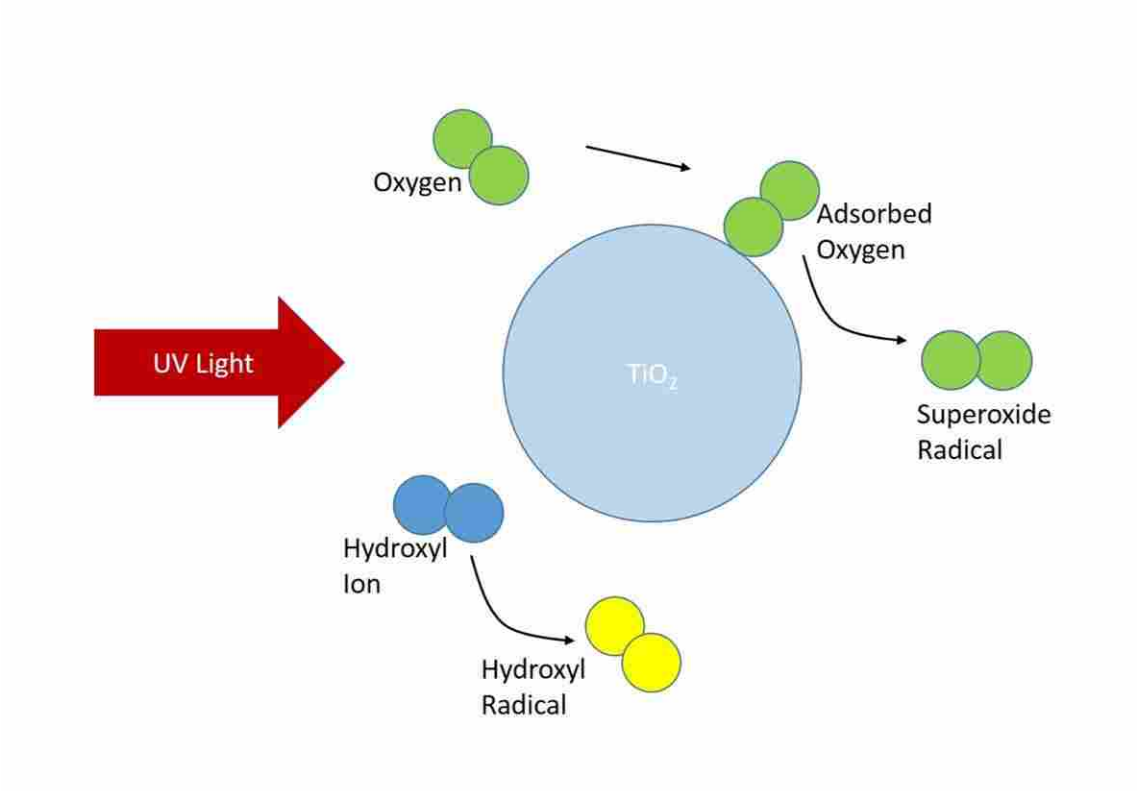

Figure 3.1: Schematic of Photocatalysis that occurs in aqueous solution (Purifics®, 2009).

3.2 Advanced Oxidation Process using TiO_2 Photocatalysis and the Photo-Cat system.

The Photo Cat system that was used for phosphorus removal in this chapter is a flexible water purification technology that has been commercially available since 1994

(Purifics®, 2009). The main advantage of the Photo Cat system is that it can support sustainable development, eliminating necessity for chemical oxidants. This system can destroy organic pollutants in wastewater by using chemical reactions, as explained earlier in this.

Other than conventional catalytic processes such as the catalytic converter on automobiles, TiO_2 in the Photo-Cat system uses UV light energy for activation as a catalyst (Purifics®, 2009). During the experiments using the Photo-Cat system, only electricity will be used. Figure 3.2 is an actual photo of the Photo-Cat system. This instrument consists of three parts: the Photo-Catalytic advanced oxidation part, the Ultra Violet irradiation part, and the ceramic membrane UF part. (Purifics®, 2009).

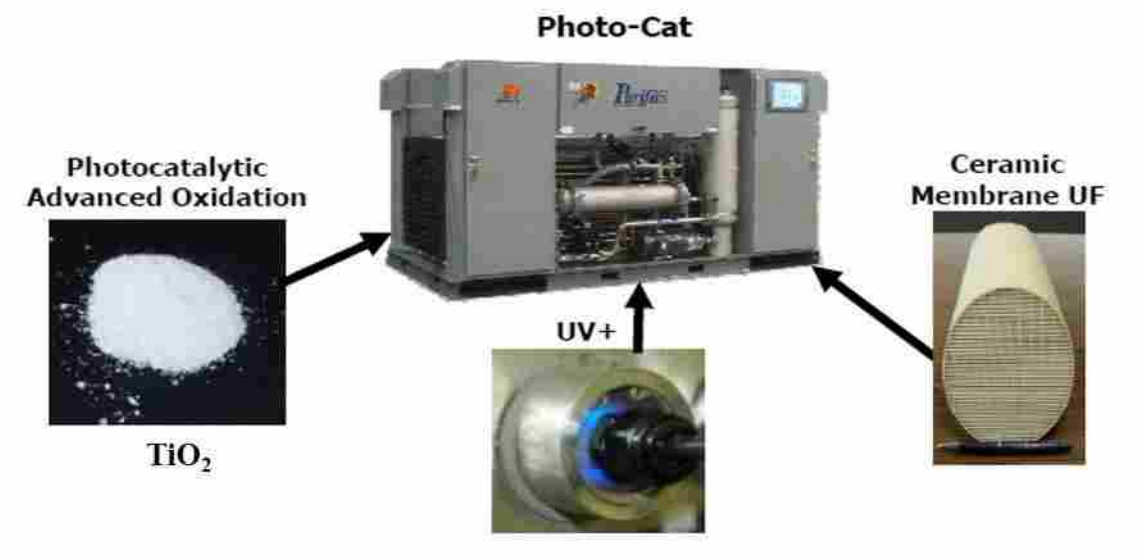

Figure 3.2: The structure of Photo-Cat system in Purifics. The Photo-Cat system (3.6m L x 1.02m W x 1.98m H) basically consists of three part as explained above (Purifics®, 2009).

3.3 Methodology

In laboratory model systems, phosphate has been shown to bind to TiO_2 nano particles with as much as 80% of phosphorus being separated to the solid surface (Kang *et al*., 2011). The Photo-Cat systems are TiO_2 based systems which can potentially remove phosphorus as currently configured, however, this needs to be tested for some parameters (e.g. pH, ionic strength). In terms of a progression of samples for testing, simple phosphate such as orthophosphate will be tested first. Then organic compounds and real wastewater samples will be tested. For inorganic phosphate removal, no UV light is necessary, however, for figuring out how the UV light works on phosphate removal, especially on organic phosphorus, UV light will be utilized to potentially convert organic phosphorus to reactive phosphate, which can be removed by surface complexation of TiO_2.

The basic method involved cycling test water through the Photo-Cat system and taking two types of sample: orthophosphate and organic phosphate. Thus, the first experiment is testing removal of reactive phosphorus (RP) in sample solutions (e.g. orthophosphate), and the second experiment is testing removal of organic phosphorus in sample solutions including real water and wastewater. To find out optimal parameters of phosphorus removal, pH, ionic strength and UV light will be discussed as dependent variables.

Phosphorus was measured using Standard Methods 4500P-E ascorbic acid method. A complete introduction and explanation of the ascorbic acid method can be found in Chapter 2.

The absorbance was measured using an auto analyzer, also known as an auto colorimeter. Synthetic Waste Water (SWW) samples that include inorganic phosphorus were directly measured by the ascorbic acid method for measuring total reactive phosphorus (tRP) without any pretreatment. However, for measuring SWW and real wastewater samples that include organic phosphorus, a digestion procedure (persulfate and heat) was used as a pretreatment for measuring total phosphorus (TP).

3.3.1 Persulfate Digestion for Total Phosphorus

For determination of total phosphorus (TP) in samples, a digestion procedure is needed because only phosphate can be measured by the colorimetric method (Smith, 2015). There are diverse digestion techniques have been used for TP determination. During the experiments, the acidic persulfate oxidation method was used. In this method, ammonium persulfate ($(NH_4)_2S_2O_8$) is used along with sulfuric acid to oxidize organic and condensed phosphorus compounds in a sample so that they can be measured as a form of reactive P (RP) by the colorimetric method (W. Maher and L. Woo, 1998; H. Gray, 2012). In persulfate digestion, the persulfate anion is reduced to the sulfate anion. The

two electrons that were donated by broken bonds of the oxidized compounds react with persulfate anions. This reaction is explained by equation 3.1 (Smith, 2015).

$$S_2O_8^{2-} + 2e^- \rightarrow 2SO_4^{2-} \text{ (Smith, 2015)} \qquad \text{(Eq.3.1)}$$

A TP digestion of a 2.5mL sample is processed by the addition of 20mg of ammonium persulfate and 100µL of 11N H_2SO_4. After that, the prepared sample is heated using HACK DRB200 digital reactor block digestor (Loveland, Colorado) for 120 minutes at 105°C. After 120 minutes, the sample is cooled to room temperature and 10µL of phenolphthalein indicator is added. Lastly, the solution is neutralized to a faint pink color by the addition of 1M of NaOH and diluted to 5mL with Milli-Q water for the colorimetric method. After this procedure, the ascorbic acid method was followed for the determination of residual phosphorus in sample using auto analyzer.

3.3.2 Dynamic Light Scattering (DLS)

Dynamic light scattering (DLS) is a technique to determine the size of particles. Specifically, DLS can show actual particle size by measuring the diffusion constant of particles suspended in solution (Kwon, 1999). This DLS technique is widely used because it has not only short measurement time but also simple operation procedure. However, if the sample solution has diverse particles in it, the measurement accuracy decreases dramatically (An, 2012).

For determination of size of particles, the Malvern DLS instrument which can measure the particle size within a range of 0.3nm to 10μm were used. The Malvern DLS instrument creates an autocorrelation function that comes from the measured fluctuations in the scattered light intensity over determined time by users. The equivalent hydrodynamic diameter of the particles can be measured from the diffusion constant by applying the Stokes-Einstein relationship (Kwon, 1999). In the Stokes-Einstein relationship, the particles are assumed to be spherical and non-permeable. In addition, by using cumulant analysis and distribution analysis, this instrument can give not only a z-average hydrodynamic diameter (d_{DLS}) and a polydispersity index (PDI) but also an intensity-weighted size distribution (Baalousha and Lead, 2012).

3.3.3 Sample Preparation

All the solutions used in the experiments were prepared from certified reagent grade chemicals, which were used without any further purification. Reaction vessels were treated with 5% HNO_3 and rinsed 2-times with Milli-Q water before they were used.

During the experiments, a synthetic wastewater (SWW) was used for measuring phosphorus removal in similar condition compared to real wastewater sample. A ph was fixed at 6 and ionic strength was varied using half salt, 1x salts and 2x salts. A SWW was made based on the recipe shown in Table 3.1 (Jung *et al*., 2005).

Table 3.1: A SWW sample basically has 5mg/L of initial phosphorus. However, samples have different reagent concentration for varying ionic strength of synthetic wastewater (Jung et al., 2005).

Used Reagents	Reagent Concentration (mg/L)
Calcium Chlroride ($CaCl_2$)	2.4
Magnesium Sulfate ($MgSO_4$)	24.0
Sodium Bicarbonate ($NaHCO_3$)	300.0
Sodium Acetate (CH_3COONa)	820.3
Potassium Phosphate (KH_2PO_4)	5.0

In order to determine the influence of pH on tap water in terms of phosphorus removal without the addition of TiO_2 nanoparticles, the basic SWW samples described in Table 3.1 were diluted with three types of water shown in Table 3.2 below. In addition, to characterize particle size at different pH, the dynamic light scattering (DLS) technique was used.

Table 3.2: For determination of effect of pH, not only the tap water from different region but also milli-Q water used for dilution of sample.

Sample Dilution	phosphorus concentration (mg/L)
SWW + London (ON) tap water	2.765mg P/L
SWW + Waterloo (ON) tap water	
SWW + Milli-Q water	

Not only synthetic organic phosphorus but also real water samples collected in Luther Marsh (stock solution with a terrestrial reverse osmosis organic matter isolate) and Speed River (43° 23′ 15″ N, 80° 22′ 1.5″ W, ON, Canada) were used. More details on Luther Marsh organic matter sample not only location but also chemical characteristics are found in a literature (Gheorghiu *et al*., 2010). Speed River sample grabbed at actual site. For making a certain amount of phosphorus in real water samples collected at local site, 1x SWW was added. For synthesizing organic phosphorus, three types of organic phosphorus found in Table 3.3 are used. Different types of organic phosphorus were used to make 5mg/L of initial phosphorus. The ionic strength is maintained by following basic synthetic wastewater recipe.

Table 3.3: Recipe for making of organic phosphorus. ATP, AEP and phytic acid are used for synthesizing wastewater samples.

Used Organic phosphorus	Reagent Concentration (mg/L)
Adenosine Triphosphate (ATP)	1.67mg/L
Aminoethyl Phosphate (AEP)	1.67mg/L
Phytic Acid	1.67mg/L

For real wastewater samples, effluent from the anaerobic membrane bio reactor (AnMBR), as well as industrial influent and effluent were used without any further treatment shown in Table 3.4. Industrial influent and effluent were from an anonymous

source and details on AnMBR is found in Gray, 2012.

Table 3.4: Real wastewater samples were used to determine phosphorus removal by Photo-Cat system. Due to the high ratio of non-reactive phosphorus (NRP) in these sample, persulfate digestion was used to determine TP.

Wastewater Collected	Phosphorus Concentration (mg/L)	Note
AnMBR Effluent	2.5-3mg P/L	Added directly as collected
Industrial influent	6 mg/L	Added directly as collected
Industrial effluent	Less than 1mg/L	Added directly as collected

For measuring TP, the digestion technique must be performed in order to convert organic phosphorus into RP for the colorimetric method. For the persulfate digestion procedure, ammonium persulfate and sulfuric acid were used. After digestion, collected samples were analyzed using an auto colorimeter (AA3, SEAL Analytical, Canada) to measure how much phosphate could be removed by putting TiO_2 nanoparticles.

3.3.4 Reagents and Materials

TiO_2 P25 (obtained from Aeroxide®) consisting of anatase and rutile with a ratio of 80:20 and having BET surface area of $50 m^2/g$ and average particle size of 21nm was used as a sorbent without further treatment in this experiment (Evonik Industry, 2015). For synthesizing a simple waste water sample (inorganic phosphorus sample),

monopotassium phosphate (KH_2PO_4, 99%, VWR, USA), calcium chloride ($CaCl_2$, 99%, VWR, USA), magnesium sulfate ($MgSO_4$, 99%, VWR, USA), sodium bicarbonate ($NaHCO_3$, 99%, VWR, USA), and sodium acetate (CH_3COONa, 99%, VWR, USA) were added to Milli-Q water (18.2MΩ, Milli-Q water) and a sample of 5mg P/L was made. For making synthetic waste water sample of organic phosphorus, AEP ($H_2N(CH_2)_2OP(O)(OH)_2$, 99%, VWR, USA), ATP ($C_{10}H_{16}N_5O_{13}P_3$, 99%, VWR, USA), and phytic acid ($C_6H_{18}O_{24}P_6$, 99%, VWR, USA) were used. Lastly, real wastewater samples were collected from Luther Marsh. During the experiments, pH was a range of 4 to10 adjusted by 1M of HCl and NaOH. Ammonium persulfate ($(NH4)_2S_2O_8$, Sigma Aldrich, USA) and sulfuric acid (H_2SO_4, VWR, USA) were used.

An auto colorimeter (AA3, SEAL Analytical) was also used for determining phosphorus concentration by the absorbance value. The mixed reagent was prepared in combination with sulfuric acid (H_2SO_4) (98+%, EMD Millipore, USA), ascorbic acid (98+%, Alfa Aesar, USA), ammonium molybdate ($H_{24}Mo_7N_6O_{24}\cdot 4H_2O$, Sigma Aldrich, USA) and potassium antimonyl tartrate ($C_8H_4K_2O_{12}Sb_2\cdot 3H_2O$, 99+%, Sigma Aldrich, USA). . The absorbance was measured with 10 mm flow-cell at 660 nm.

For characterization of precipitation and determination of particle size in tap water samples, Zetasizer Nano ZS (Melvern Instruments, U.K) was used.

3.4 Result and Discussion

In Chapter 2, phosphorus adsorption onto TiO_2 mixed bulk powder is presented in Figure 2.10 and that showed approximately 27% of bound phosphorus to the surface. In this chapter, TiO_2 nanoparticles will be discussed. TiO_2 nanoparticles are used as an adsorbent, and are known for their huge surface areas. Thus, more phosphorus removal is expected when using nanoparticles than when using bulk powder due to the high binding capacity of nanoparticles. In Figure 3.3, as expected, maximum phosphorus removal was achieved approximately 100% at pH around 10, which is much higher than the maximum phosphorus removal with TiO_2 bulk powder. However, the trends of pH dependence for nanoparticles seem to be inversed in comparison with the trend with bulk powder. Thus, the trend of nanoparticles may also be related to other significant parameters such as ionic strength or choice of tap water for dilution of sample.

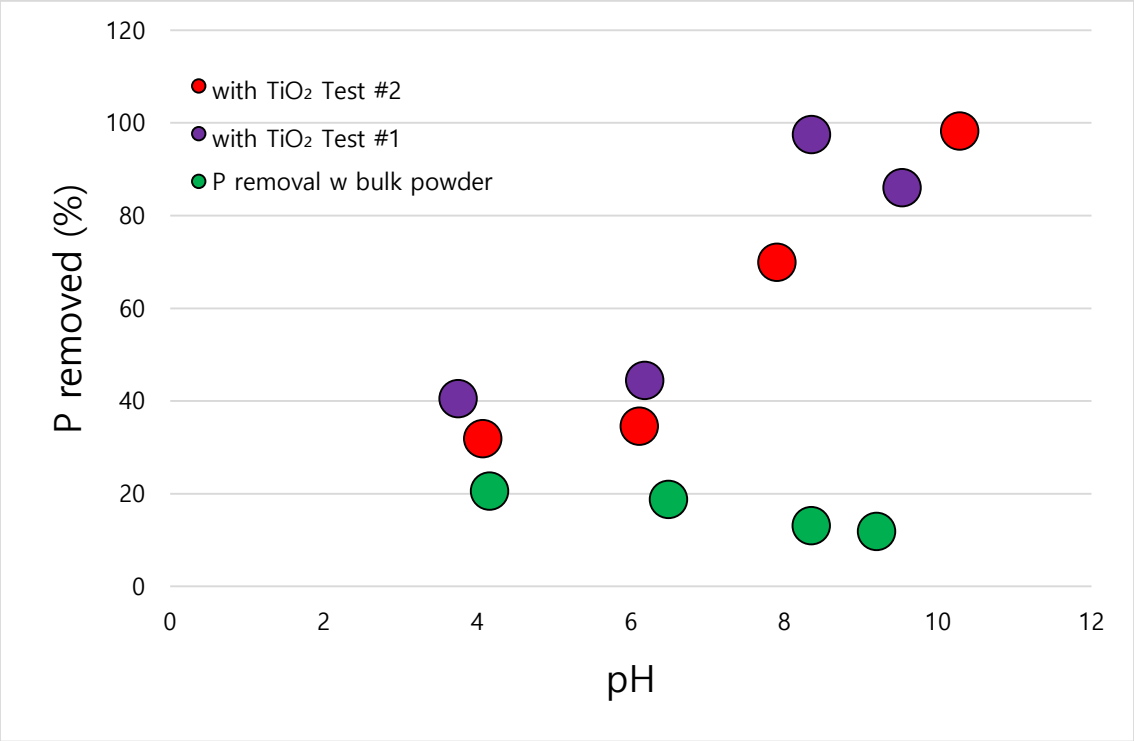

Figure 3.3: Percent phosphorus removal at different pH. In terms of phosphorus removal, TiO_2 nanoparticles show much higher removal than bulk powder with inversed pH dependence. Based on the recipe in Table 3.1, phosphorus represents orthophosphate in this test.

3.4.1 The Influence of Ionic Strength and pH for Phosphorus Removal

For determination of the optimal phosphorus removal conditions of the Photo-Cat system, ionic strength, acetate, and pH were taken into account as dependent variables.

In Figure 3.4, it can be found that phosphorus removal is not affected by salt concentration of the synthetic wastewater. The result of both test 1 and 2 shows no specific trends or significant difference in phosphorus removal. Thus, it is clear that ionic strength is not a dependent variable to determine the optimal condition of phosphorus removal using TiO_2 nanoparticles.

Acetate was used for proton competition. If acetate work as expected, phosphorus removal will be decreased. However, in Figure 3.5, no changes can be observed between sample with acetate and without acetate. Thus, like ionic strength, acetate turned out that it is not a dependent variable in this chapter.

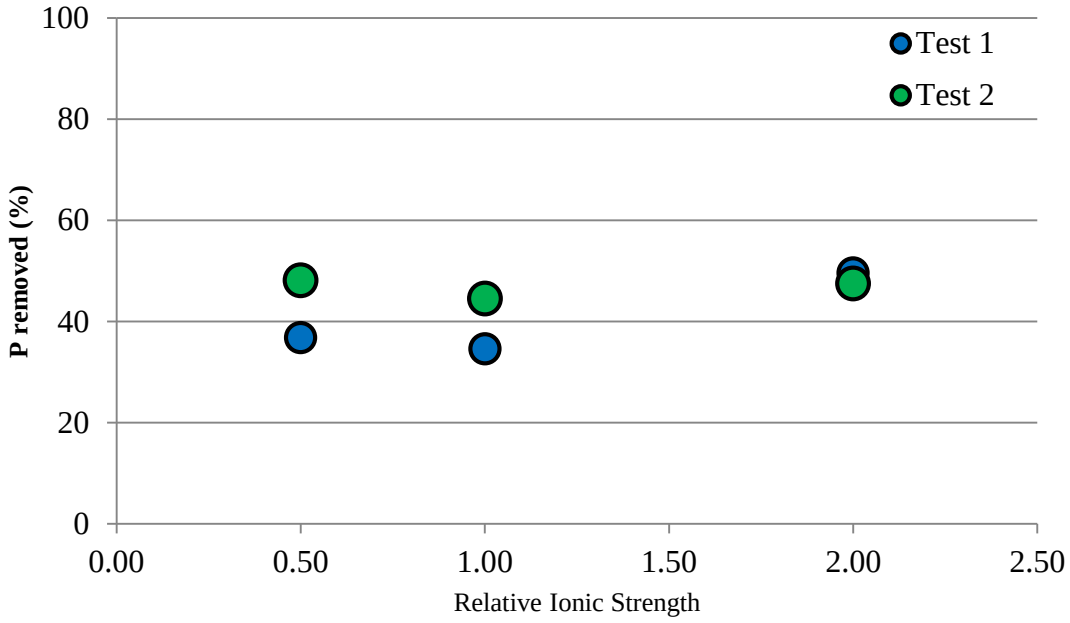

Figure 3.4: Percent phosphorus removal versus ionic strength of synthetic wastewater sample. Both test 1 and 2 do not show a huge difference and any trends in terms of phosphorus removal. SWW were made based on Table 3.1.

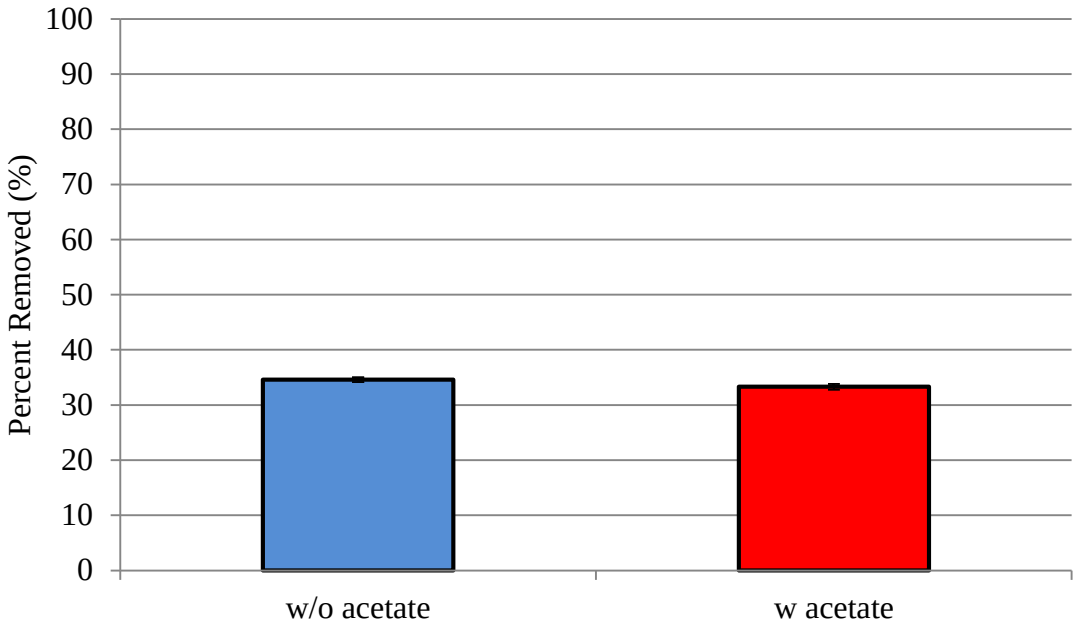

Figure 3.5: Percent phosphorus removal with and without acetate in samples. There is no difference between blue (34% of phosphorus removal) and red bar (33% of P removal) in terms of phosphorus removal. SWW were made based on Table 3.1.

In terms of pH dependence, phosphorus removal occurred in the Photo-Cat system with increasing pH with or without the addition of TiO_2 nanoparticles. Phosphorus removal tests with TiO_2 nanoparticles could achieve more than 90% of phosphorus removal on average as shown in Figure 3.6. Interestingly, below pH 8, less than 12% of phosphorus was removed just by pH adjustment without the addition of TiO_2 nanoparticles. However, above pH 10, it is observed that approximately 60% of phosphorus was removed. Thus, more ideas and experiments should be considered to determine phosphorus uptake without TiO_2 nanoparticles.

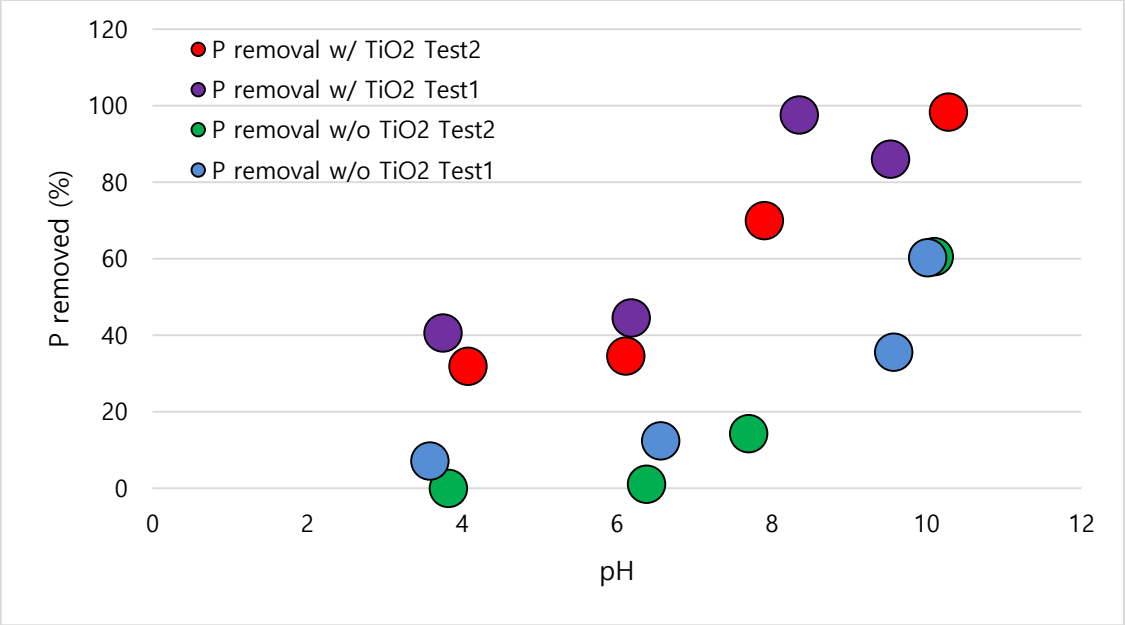

Figure 3.6: A percentage of removed phosphorus onto TiO_2 nanoparticles. It is shown that even without TiO_2 nanoparticles, phosphorus in London tap water seems to be removed in this Figure.

3.4.1.1 The Effect of pH on Phosphorus Removal in Tap Water

Interestingly, in Figure 3.3, inversed pH dependence trend is observed compared to pH dependence with TiO_2 bulk powder. In addition, phosphorus removal was achieved even without the addition of TiO_2 nanoparticles. Thus, for determination of this opposite of expectation, a few testable hypothesizes have to be cleared.

1. Can ceramic membrane filter remove phosphorus?
2. Can in situ generation of Ca-P or Mg-P precipitates influence phosphorus removal?

The Photo-Cat system has its own functional membrane filter, which is made of alumina that is known to remove phosphorus but has pH dependence (Tanada *et al*., 2003).

Thus, as pH changes, phosphate might bind to the ceramic membrane filter. In addition, tap water that was used during the tests to dilute samples could also influence phosphorus removal because general tap water usually contains various constituents in itself, such as Ca^{2+}, Mg^{2+}.

Several tests were performed in order to demonstrate an effect of tap water without the addition of TiO_2 nanoparticles for achieving phosphorus removal. Samples' pH varied from 2 to 10 while including 2.76mg P/L. Samples were diluted with Milli-Q water, tap water from London, and tap water from Waterloo.

In Figure 3.7, all the samples at pH from 2.2 to 9.9 without TiO_2 nanoparticles show no phosphorus removal with the exception of the tap water from London with approximately 56% phosphorus removal at around pH 10. According to previous research, reactions between minerals such as Mg^{2+} or Ca^{2+} and phosphate can form struvite or apatite at various pH value (Kim, 2004; Hao *et al*., 2008; Turker and Celen, 2010). In addition, it was reported in literature (Song *et al*., 2002) that precipitation between calcium and phosphate to produce calcium salt in a sample.

In Figure 3.8, solubility of calcium phosphates was plotted under the assumption that concentration of Ca^{2+} is 36 mg/L (i.e. actual Ca^{2+} concentration measured by ICP was approximately 36 mg/L). Based on this Figure 3.8, supersaturated

point of calcium phosphates can be determined. For example, above pH 6, apatite starts to be supersaturated and above pH 7.5, $Ca_4H(PO_4)_3$ starts to be supersaturated (phosphate represented with yellow line).

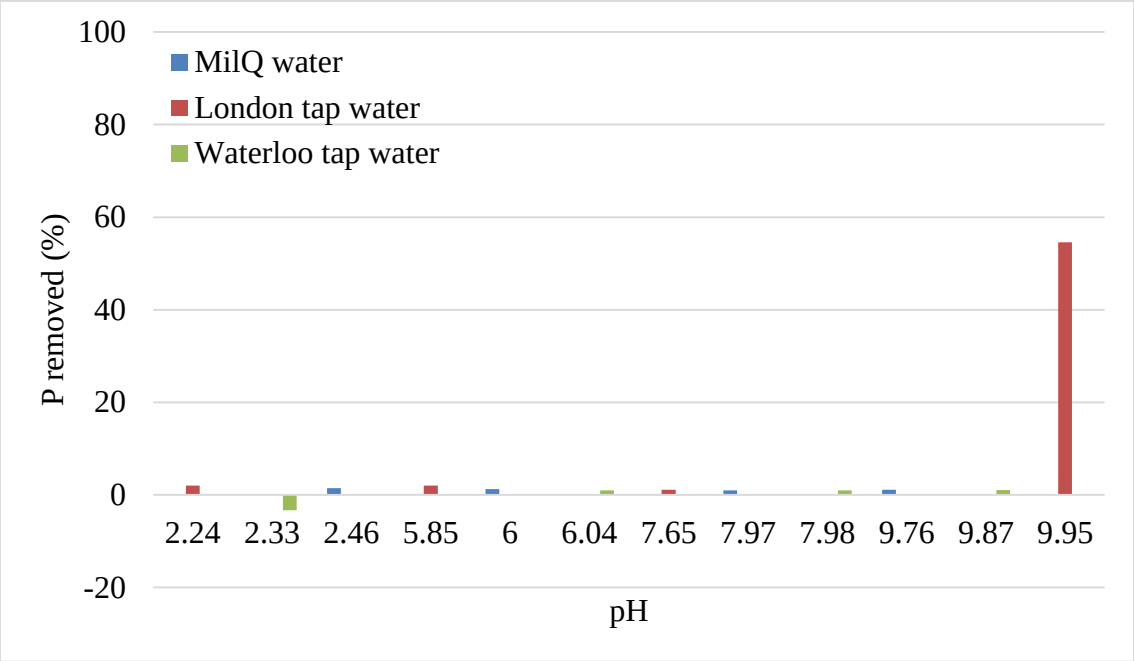

Figure 3.7: A percent removed phosphorus without the addition of TiO_2 nanoparticles. During the test, only the London tap water shows approximately 56% of phosphorus removal at pH 10.

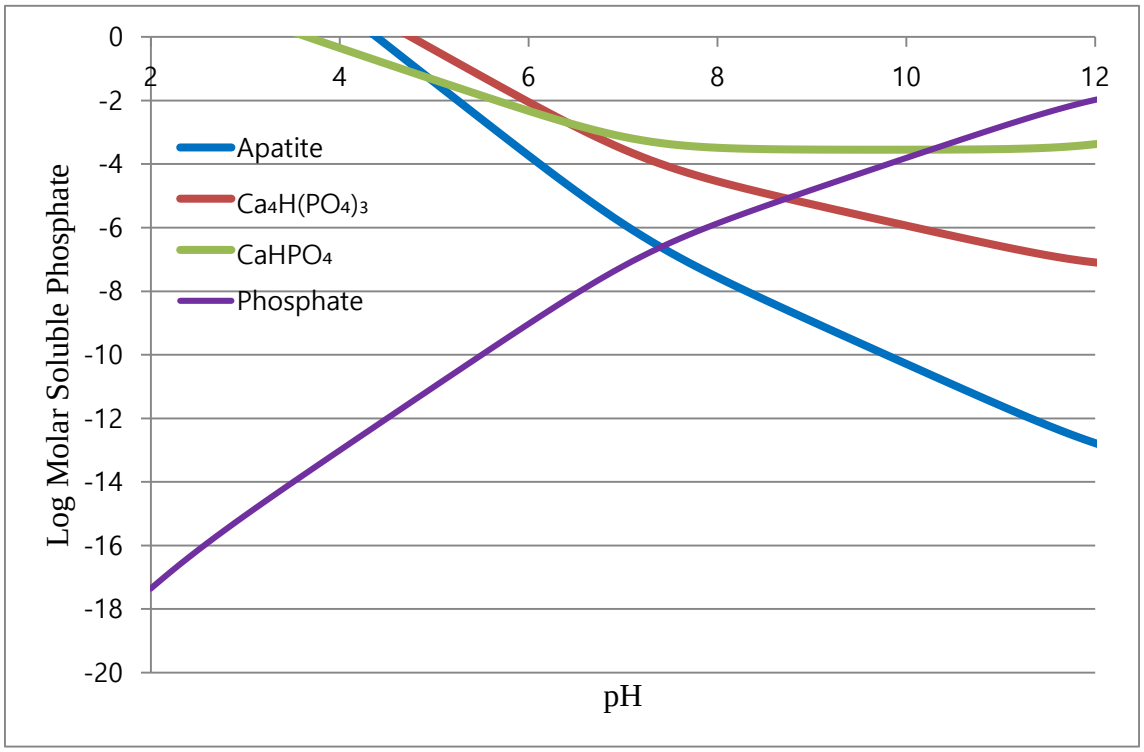

Figure 3.8 Solubility of calcium phosphates. The solubility of calcium phosphate phases has been calculated under the assumption that [Ca^{2+}] = 36 mg/L.

Dynamic light scattering (DLS) techniques are well known for characterization of particle size. Thus, to clarify the actual particle size of apatite in the tap water sample, the Zetasizer, which can measure particle size using the principle of DLS was used. In Figure 3.9, the tap water from London shows a much larger diameter at pH 10, that is around 6.9 μm. The particle size of the other samples was much smaller, approximately 0.9-2.0 μm. This can explain phosphorus removal at pH 10 without the addition of TiO_2 nanoparticles. At pH 10, the London tap water seems to have a high enough concentration of minerals (e.g. Ca^{2+}) compared to other samples. A particle size of 6.9 μm is more than two times larger than the others' average size. Thus, this size

difference between low pH and high pH may be a demonstration of precipitation such as apatite, or calcium phosphate.

Moreover, the Zetasizer can give other values to characterize detected particles, such as attenuator. Due to particles' density in sample, a laser beam used as a light source can be scattered. In Table 3.5, relationship between the attenuator index and transmission value is shown. Based on Table 3.5, density of particles in sample can be determined. That is, if attenuator value is 11, which means 100% transmissivity, the sample has no particles to interrupt light penetration.

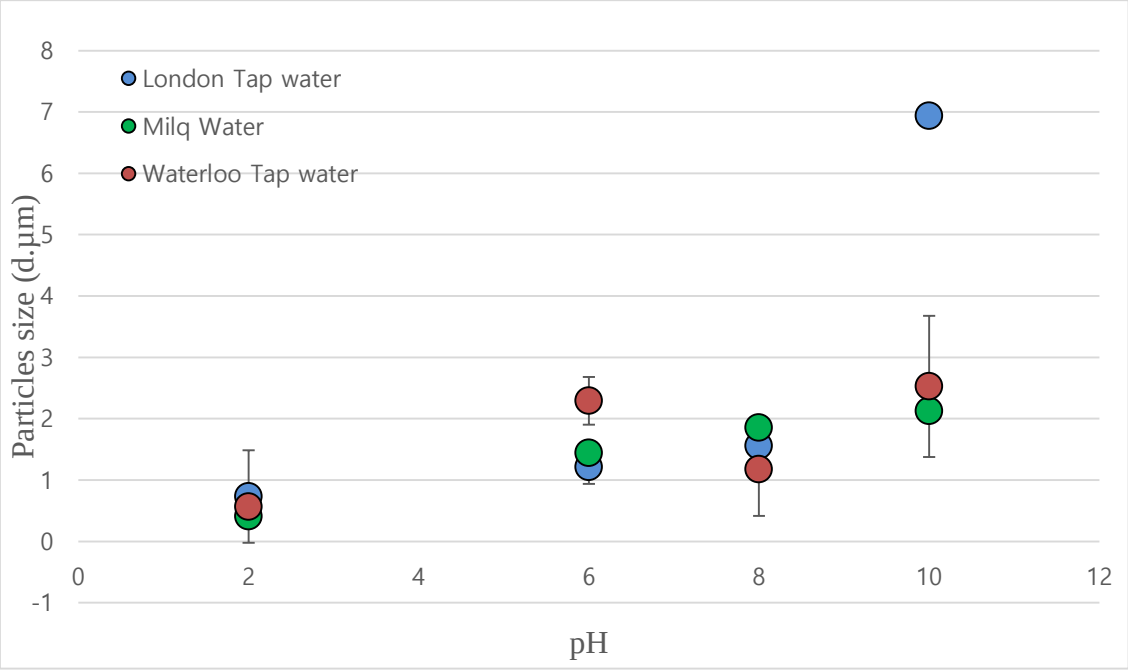

Figure 3.9 An average particle size measured using the Zetasizer with pH range of 2-10.

Table 3.5: Relationship between the attenuator index and transmission value (adapted from Zetasizer nano series manual, 2013).

Attenuator Index	Transmissivity (% Nominal)
1	0.0003
2	0.003
3	0.01
4	0.03
5	0.1
6	0.3
7	1
8	3
9	10
10	30
11	100

In Table 3.6, only London tap water at pH 10 shows different attenuator value, which is 8. This means more particles are present in this sample. Since a value of 11 represents 100% transmissivity, it seems that all samples except London tap water at pH

10 have few particles which allow laser beam to penetrate each sample without light being scattered.

Table 3.6: Attenuator index for each sample at various pH values. London tap water at pH 10 shows value of 8.

Sample name	pH	Attenuator index
London tap water	2	11
	6	11
	8	11
	10	8
Waterloo tap water, Milli-Q water	2	11
	6	11
	8	11
	10	11

For the demonstration of mineral precipitation or coagulation, actual mineral concentration in both London and Waterloo tap water were measured by ICP-OES (Inductively Coupled Plasma Optical Emission Spectroscopy). It turned out that London tap water contains 36.18 mg/L of calcium, whereas, calcium constituent of Waterloo tap water was 0.87 mg/L. That is, calcium concentration in London tap water is approximately 41 times higher than that of Waterloo tap water. Thus, due to high

calcium concentration, much phosphorus in London tap water react with calcium to produce calcium phosphates at high pH like 10. As Figure 3.7 is plotted based on [Ca^{2+}] of 36 mg/L, at pH 10, London tap water should be supersaturated. In addition, phosphorus removal without the addition of TiO_2 nanoparticles can be explained by production of calcium phosphates.

3.4.2 Various Parameters for Real Water regarding Phosphorus Removal

The Advanced Oxidation Process (AOP) is the technology utilized in the Photo-Cat system by using free hydroxyl radicals (●OH) as a strong oxidant to break down organic phosphorus in wastewater (Metcalf & Eddy, 2003). In the Photo-Cat system, free hydroxyl radicals can be formed by irradiation of UV light. Thus, basically organic P can be converted into phosphate. Once phosphate is formed after irradiation of UV light, it may bind to the TiO_2 nanoparticles to form surface complexation or be removed by mineral precipitate (see above).

In Figure 3.10, among four types of sample including synthetic organic phosphorus and real water, not much difference is observed between the result with UV light and without UV light in terms of phosphorus removal.

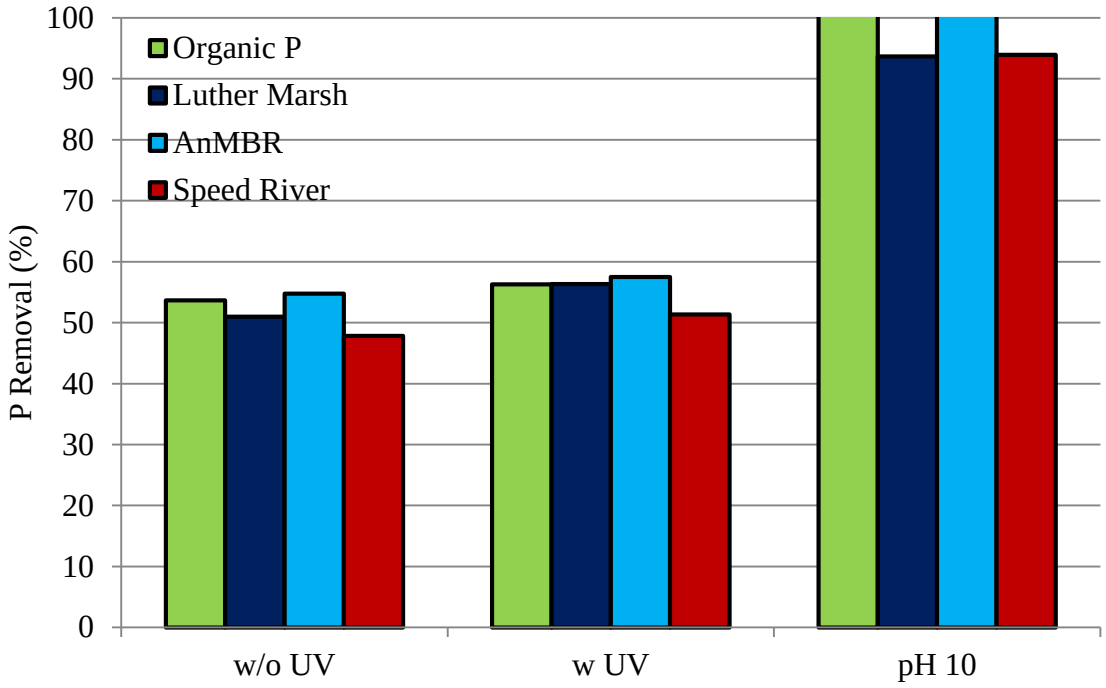

Figure 3.10 A comparison of phosphorus removal with UV light and without UV light at pH 6, and with pH 10. TiO_2 nanoparticles were added into the Photo-Cat system before measuring. All samples shown in this graph contain more than 90% of RP except organic phosphorus. Thus, majority of removed phosphorus during this test was thought to be RP (e.g. orthophosphate).

Samples irradiated by UV light do not show any significant difference in terms of phosphorus removal. The explanation could be that UV light does not actually convert organic phosphorus into RP with photo-oxidation as expected. However, interestingly, pH adjustment to 10 showed over 90% of phosphorus removal in every sample. The influence of pH adjustment on phosphorus removal on tap water was demonstrated in section 3.4.1.1, and all samples added into Photo-Cat system were diluted with tap water (London). Thus, by adjustment of pH, minerals such as calcium

or magnesium could be bound to phosphate to form a precipitation causing phosphorus uptake in samples.

The effect of the ceramic membrane filter in the Photo-Cat system was revealed by using two real wastewater samples (referred to as plant effluent and industrial wastewater) collected at an anonymous water pollution control plant. Before running the Photo-Cat system, initial TP was measured by ICP to determine how much TP could be removed by using the ceramic membrane filter. Collected real wastewater samples were directly poured into the Photo-Cat system and not diluted with tap water. Thus, the ceramic membrane filter should be the only parameter to be taken account of.

In Figure 3.11, red and blue bar represent percent phosphorus removal and green and yellow dot represent phosphorus concentration in samples. In this graph, the ceramic membrane filter shows 36-45% of phosphorus removal on industrial wastewater. TiO_2 nanoparticles and UV light turned out not to influence phosphorus removal on industrial wastewater.

Interestingly, TiO_2 nanoparticles and UV light seem to affect to phosphorus removal on plant effluent sample in the aspect of phosphorus removal efficiency. Ontario regulation for this anonymous plant are for an average TP of 0.3 mg/L, thus the Photo-Cat system can remove phosphorus to below permitted value (0.3 mg P/L).

Based on Figure 3.12, high amount of non-reactive P (NRP) can be found in industrial wastewater. Unlike SWW samples used in this chapter, real wastewater sample considered to contain much non-reactive phosphorus in it. Although synthetic organic phosphorus sample showed phosphorus removal with TiO_2 nanoparticles, non-reactive phosphorus in real wastewater could not be removed by adding TiO_2 nanoparticles nor UV light. It seems that the NRP in this industrial influent might be very refractory phosphorus (e.g. phosphonates) compared to reactive phosphorus and thus be difficult to remove.

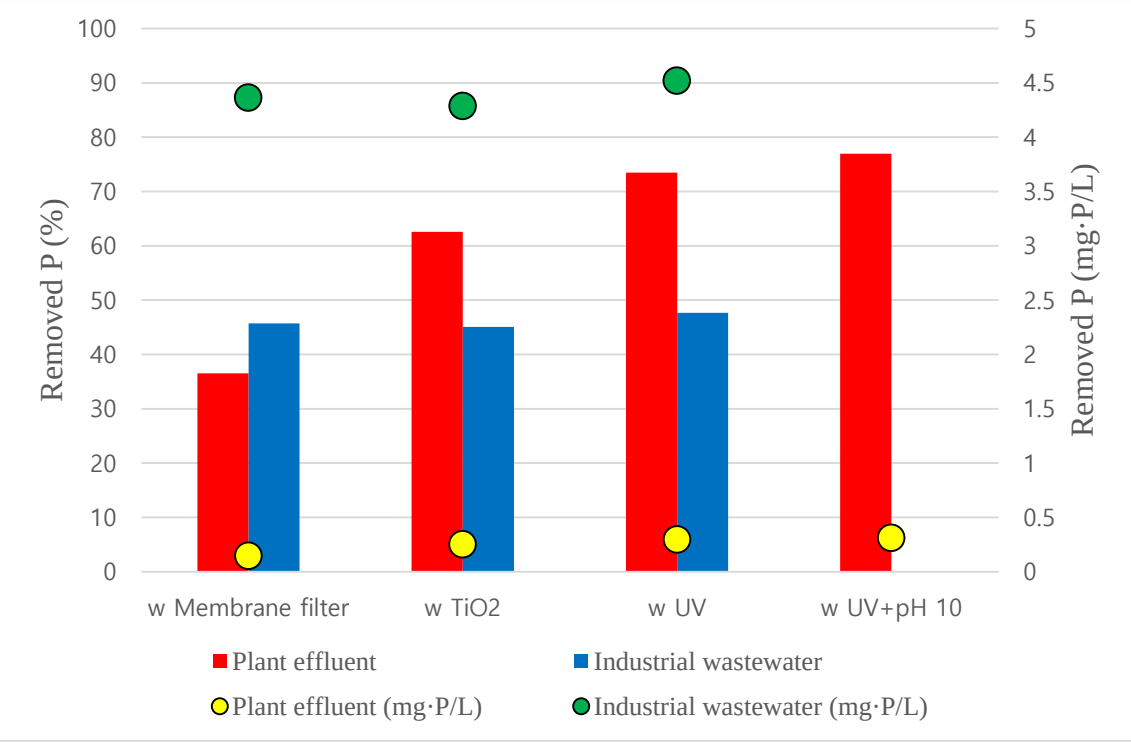

Figure 3.11 The y axis on left side represents percent removed phosphorus correspond to red and blue bars whereas the value on right side represents removed phosphorus concentration correspond to green and yellow dot. As a value of initial pH of industrial wastewater was around 10, pH adjustment was not needed.

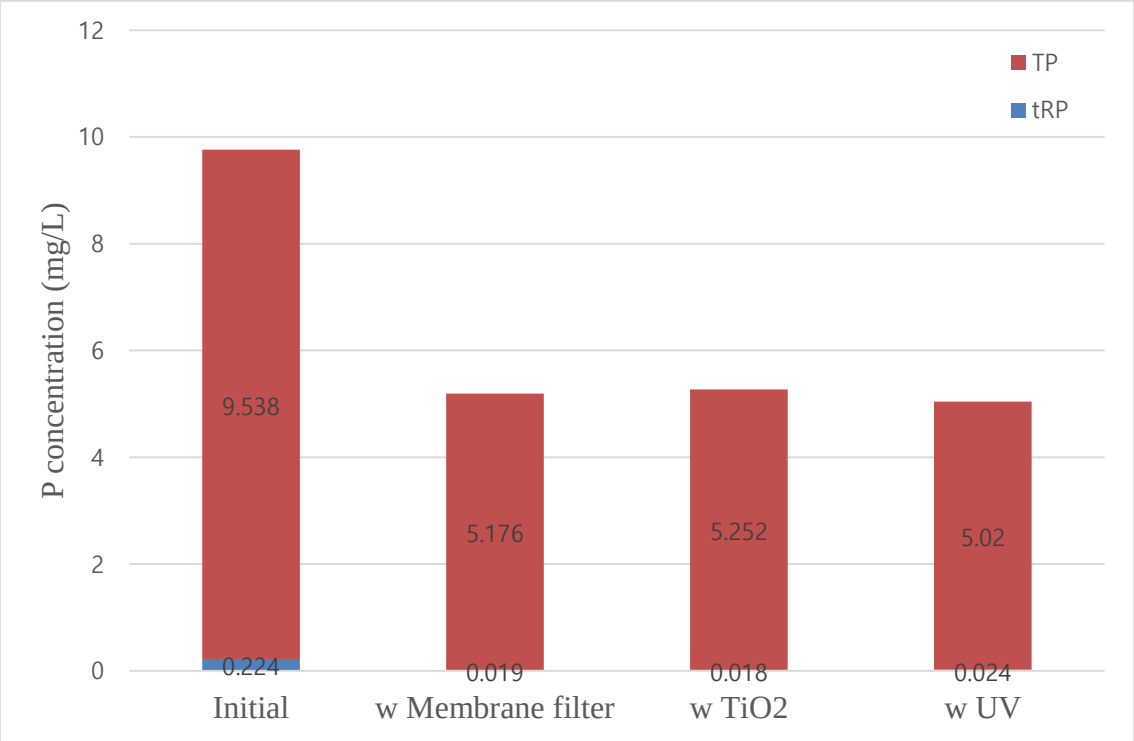

Figure 3.12: A comparison between TP and tRP. A real wastewater sample thought to contain much NRP (e.g. phosphonate) compared to other samples used in this chapter. The gap between red bar and blue bar should be NRP in this Figure. Approximately 37% of TP (including NRP) seems to be removed by the ceramic membrane filter.

3.5 Conclusion

The investigation to optimize efficient condition for phosphate removal by TiO_2 nano particles with using Photo-Cat system was performed in this chapter. The possible parameters for phosphorus removal by TiO_2 nanoparticles were ionic strength, acetate, sample's pH, effect of tap water, and the ceramic membrane filter.

An ionic strength varied half salt, 1x salt, and 2x salt as a relative ionic strength based on the recipe (Jung *et al*., 2005). To observe any phosphate competition by acetate,

acetate also added. The result shows that there was no huge gap among different ionic strength in terms of phosphorus removal and the addition of acetate did not show any gap. It seems that an ionic strength and acetate do not need to be considered as a parameter.

A pH dependence of phosphorus removal using TiO_2 which confirmed in previous chapter also found using nanoparticles. However, using Photo-Cat system, inversed phosphorus removal trend was observed in comparison with the previous result. As tap water was used for dilution of synthetic wastewater sample, the investigation for effect of tap water was fulfilled. Interestingly, tap water used for Photo-Cat system shows similar trend in terms of phosphorus removal without the addition of TiO_2 nanoparticles. During the investigation, Milli-Q water and tap water collected at London, Ontario (used for Photo-Cat system) and Waterloo, Ontario were used. Tap water generally contains minerals such as Ca^{2+} and Mg^{2+} as major constituents. In previous research, calcium phosphate and apatite shows similar pH dependence trend was reported, thus, it seems that tap water collected at London contains higher calcium concentration compared to Waterloo tap water and Milli-Q water. Average particle size in each tap water and Milli-Q water measured by the Zetasizer could also demonstrate the difference. The Zetasizer shows London tap water at pH 10 has much particle in it and its size also much larger than the other samples' particle size.

In terms of phosphorus removal of real wastewater sample, TiO_2 nanoparticles seems not to remove nonreactive phosphorus. However, the ceramic membrane filter shows 38% of phosphorus removal.

In summary, TiO_2 nanoparticles can remove RP as well as synthetic organic phosphorus during the investigation. However, anthropogenic phosphorus (e.g. NOP) can't be removed by TiO_2 nanoparticles using Photo-Cat system. And ceramic membrane filter that utilized in Photo-Cat system could achieve efficient phosphorus removal and majority of removed phosphorus is considered to NOP.

3.6 References

An. S. H. (2012). An efficient particle size distribution estimation method for dynamic light scattering system using modified penalized least square. Master's Thesis, Ewha Womans University, Seoul, Republic of Korea.

Evonik Industry. (2015). Technical information 1243: AEROXIDE®, AERODISP® and AEROPERL® Titanium Dioxide as Photocatalyst. Etobicoke, ON, Canada.

Baalousha. M., Lead. J. R. (2012). Rationalizing nanomaterial sizes measured by atomic force microscopy, flow field-flow fractionation, and dynamic light scattering: Sample's preparation, polydispersity, and particle structure. *Environment Science Technology, 2012, 46,* 6134-6142.

Choi. J. (2013). Titanium oxide based photocatalysts for highly efficient hydrogen gereration. Master's Thesis, Korea University, Seoul, Republic of Korea.

Fujishima, A., Honda, K. (1972). Electrochemical photolysis of water at a semiconductor electrode. *Nature 238*, 37-38.

Gray, H. (2012). Laboratory methods for the advancement of wastewater treatment modeling. Master's Thesis, Wilfrid Laurier University, Waterloo, ON, Canada.

Hao. X. -D., Wang. C. -C., Lan. L., Van Loosdrecht. M. C. M. (2008). Struvite formation, analytical methods and effects of pH and Ca^{2+}. *Water Science & Technology, 58.8*, 1687-1692, doi: 10.2166/wst.2008.557

Hashimoto. K., Irie. H., Fujishima. A. (2005). TiO_2 Photocatalysis: A historical overview and future prospects. *Japanese Journal of Applied Physics, Vol. 44, No. 12*, 8269-8285.

Jung. Y., Koh. H., Shin. W., Sung. N. (2005). Wastewater treatment using combination of MBR equipped with non-woven fabric filter and oyster-zeolite column. *Environment Engineering Research, Vol. 10, No. 5*, 247-256.

Kang, S. A., Li, W., Lee, H. E., Phillips, B. L., Lee, Y. J. (2011). Phosphate Uptake by TiO_2: Batch studies and NMR spectroscopic Evidence for Multisite Adsorption. *Journal of Colloid and Interface Science 364*, 455-458.

Kim. W. (2004). Phosphate removal model by calcium ion and oyster shell powder. Master's thesis, Yonsei University, Seoul, Republic of Korea.

Kwon. S. Y. (1999). Study of phase separation and critical phenomena of michellar solutions by laser light scattering. Master's Thesis, Korea Advanced Institute of Science and Technology, Daejon, Republic of Korea.

Lim. J. (2013). Preparation and characterization of nanostructured TiO_2 based photocatalysts for environmental and energy applications. Doctoral Thesis, Seoul National University, Seoul, Republic of Korea.

Maher, W., Woo, L. (1998). Procedures for the storage and digestion of natural waters for the determination of filterable reactive phosphorus, total filterable phosphorus and total phosphorus. *Analytica Chimica Acta* 375, 5-47.

Malvern Instruments. (2013). Zetasizer nano series user manual. Retrieved from http://www.chem.uci.edu/~dmitryf/manuals/Malvern%20Zetasizer%20ZS%20DLS%20user%20manual.pdf

Metcalf and Eddy, Inc. (2003). Wastewater Engineering: Treatment and Reuse, 4th edition. McGraw Hill international edition, New York, USA.

Noh. H. (2003). Studies on the photocatalytic treatment with TiO_2 and the effect of addition for phenol wastewater. Master's Thesis, Ewha Womans University, Seoul, Republic of Korea.

Purifics®. (2009). Technology briefing: Photo-Cat multi barrier water purification. London, ON, Canada. Retrieved from http://www.gitpr.com/upload/ Briefing%20-%20 Photo-Cat%20Technology.pdf

Parker, W. & Smith, S., Gray, H. (2015). State of Knowledge of the Use of Sorption Technologies for Nutrient Recovery from Municipal Wastewaters, *Water Intelligence Online* **14**.

Smith, S. (2015). Phosphorus analysis in wastewater: best practices, International Water Association, VOL. 15, 2016, doi:2166/9781780407807.

Song. Y., Hahn. H. H., Hoffmann E. (2002). The effects of pH and Ca/P ratio on the precipitation of calcium phosphate. Chemical Water and Wastewater Treatment VII, Proceedings of the Gothenburg Symposium, 10th, Gothenburg, Sweden, IWA Publishing London, 349-356.

Tanada, S., Kabayama, M., Kawasaki, N., Sakiyama, T., Nakamura, T., Araki, M., and Tamura, T. (2003). Removal of phosphate by aluminium oxide hydroxide. *Journal of Colloid and Interface Science 257*, 135-140.

Turker. M., Celen. I. (2010). Chemical equilibrium model of struvite precipitation from anaerobic digester effluents. *Turkish Journal of Engineering Environment Science 34*, 39-48, doi: 10.3906/muh-1008-15

Yang. W. M. (2006). A study on the performance and service life of coatings using photocatalyst TiO_2. Master's Thesis, Seoul National University of Technology, Seoul, Republic of Korea.

3.7 Appendix A: Supplementary Information for Chapter 2

A.1. MATLAB™ script used to simulate surface complexation model for phosphate adsorption onto TiO_2.

```
function PP=Captain_choi_TiO2s_boundphosphate_varypH
clear; Figure(1); clf; Figure(2); clf; Figure(3);clf

%%%%%%%%%%%%%%%%%%%%%%%%%%%%%%%%%%%%%%%%%%%%%%%%%%%%%%%%%%%%%%%%%%%%%55
pH=4:0.01:10.0;
PT=(6.458 * 10^-5)  ; % total phosphate
%PT=1e-18;
ASF=1.3;
TiT=(2.51 * 10^-4); % TiO2
TiT=ASF*TiT;
%TiT=1e-18;
PH=[3.95    4.2 5.6 5.97    8   8.18    9.6 10
];
BP=[1.6E-05 1.42073E-05 1.35615E-05 1.32709E-05 9.94511E-06 1.15596E-
05 1.14304E-05 9.88053E-06
];

%%%%%%%%%%%%%%%%%%%%%%%%%%%%%%%%%%%%%%%%%%%%%%%%%%%%%%%%%%%%%%%%%%%%%%

[species,names]=determine_species(TiT,PT,pH);

for i=1:size(pH,2)
for j=1:size(species,2)
       txt=[names(j,:),'(i)=species(i,j);'];
       eval(txt)
end
end

%%%%%%%%%%%%%%%%%%%%%%%%%%%%%%%%%%%%%%%%%%%%%%%%%%%%%%%%%%%%%%%%%%%%%%
%%
Figure(1);
```

```
plot(pH,TiO,pH,TiOH,pH,TiOH2)
set(gca,'fontsize',14,'linewidth',2)
xlabel('pH','fontsize',14)
ylabel('[species] (mol/L)','fontsize',14)
legend('TiO^-','TiOH','TiOH_2^+','location',
'SouthOutside','orientation','horizontal' )

Figure(2)
plot(pH,PO4,pH,HPO4,pH,H2PO4,pH,H3PO4)
set(gca,'fontsize',14,'linewidth',2)
xlabel('pH','fontsize',14)
ylabel('[species] (mol/L)','fontsize',14)
legend('PO_4^3-','HPO_4^2-','H_2PO_4^-','H_3PO_4','location',
'SouthOutside','orientation','horizontal' )

Figure(3)
plot(pH,(TiOPO3+TiO2PO2+TiO2POOH),'b',pH,PT,'r-','linewidth',2)
hold on
plot(pH,(TiOPO3),'b--','linewidth',2)
plot(pH,(TiO2PO2),'r--','linewidth',2)
plot(pH,(TiO2POOH),'g--','linewidth',2)
plot(pH,ones(size(pH))*PT,'r-','linewidth',2)
set(gca,'fontsize',14,'linewidth',2)
xlabel('pH','fontsize',14)
ylabel('[species] (mol/L)','fontsize',14)
legend('Bound P','Total P','location',
'SouthOutside','orientation','horizontal' )
axis([4 10 0 6.6*10^(-5)])
hold on;
plot(PH,BP,'ko','markersize',5,'markerfacecolor','b')
set(gca,'linewidth',2,'fontsize',14)


%%%%%%%%%%%%%%%%%%%%%%%%%%%%%%%%%%%%%%%%%%%%%%%%%%%%%%%%%%%%%%%%%%%%%%%%%%%%
%%5

save species.txt species -ascii
```

```
end

function [II,GG]=determine_species(TiT,PT,pH)

warning('off')


[KSOLUTION,KSOLID,ASOLUTION,ASOLID,SOLUTIONNAMES,SOLIDNAMES]=get_equil
ib_defn;

numpts=size(pH,2);
Ncp=size(ASOLID,1);
solid_summary=zeros(numpts,Ncp);

for i=1:size(SOLIDNAMES,1)
    txt=[SOLIDNAMES(i,:),'=zeros(numpts,1);']; eval(txt)
end

for i=1:size(pH,2)

    % adjust for fixed pH


[Ksolution,Ksolid,Asolution,Asolid]=get_equilib_fixed_pH(KSOLUTION,KSO
LID,ASOLUTION,ASOLID,pH(i));

    Asolid_SI_check=Asolid; Ksolid_SI_check=Ksolid;

    % number of different species
    Nx=size(Asolution,2); Ncp=size(Asolid,1); Nc=size(Asolution,1);

    % initial guess
    iterations=1000; criteria=1e-16;
    %%%%%%%%%%%%%%%%%%%%%%%%%%%%%%%%%%%%%%%%%%%%%%%%%%%%%%%%%%%%%%%%%%%%
%%%%%%%%%
    T=[TiT TiT PT]; guess=T./10;
```

```
    %%%%%%%%%%%%%%%%%%%%%%%%%%%%%%%%%%%%%%%%%%%%%%%%%%%%%%%%%%%%%%%%%%%%%%%
%%%%%%%%%%%%%

    % calculate species using NR

    solids=zeros(1,Ncp);

    if i==1;
[species,err,SI]=NR_method_solution(Asolution,Asolid,Ksolid,Ksolution,
T',[guess(1:Nx)]',iterations,criteria); end
    if i>1;

[species,err,SI]=NR_method_solution(Asolution,Asolid,Ksolid,Ksolution,
T',[species(2:Nx+1)],iterations,criteria);
    end

    for qq=1:Ncp

        [Y,I]=max(SI);

        if Y>1.000000001
            Iindex(qq)=I;
            Asolidtemp(qq,:)=Asolid_SI_check(I,:); %'MOH2s','NiCO3s'
            Ksolidtemp(qq,:)=Ksolid_SI_check(I,:);
            solidguess(qq)=T(I)*0.5;
           % solidguess(qq)=min(T)*0.015;
            if i>1;
                %if max(solids)>0
                txt=['solidguess(qq)=',SOLIDNAMES(I,:),'(i-1);'];
eval(txt);
                %end
            end
            guess=[species(2:Nx+1)' solidguess];

[species,err,SItst,solids]=NR_method(Asolution,Asolidtemp',Ksolidtemp,
Ksolution,T',guess',iterations,criteria);
             for q=1:size(solids,1);
```

```
            txt=[SOLIDNAMES(Iindex(q),:),'(i)=solids(q);']; eval(txt)
        end
    end

    Q=Asolid*log10(species(2:Nx+1)); SI=10.^(Q+Ksolid); Ifirst=I;

end

Q=Asolid*log10(species(2:Nx+1)); SI=10.^(Q+Ksolid);
SI_summary(i,:)=SI;

species_summary(i,:)=species;
mass_err_summary(i,:)=(err(1));

Asolidtemp=[]; Ksolidtemp=[];

end

for i=1:size(species_summary,2)
    txt=[SOLUTIONNAMES(i,:),'=species_summary(:,i);']; eval(txt)
end
%%%%%%%%%%%%%%%%%%%%%%%%%%%%%%%%%%%%%%%%%%%%%%%%%%%%%%%%%%%%%%%%%%%%%%%%%%%%
II=[species_summary dummy];
%%%%%%%%%%%%%%%%%%%%%%%%%%%%%%%%%%%%%%%%%%%%%%%%%%%%%%%%%%%%%%%%%%%%%%%%%%%%
GG=strvcat(SOLUTIONNAMES,SOLIDNAMES);


end

% -------------------- NR method solids present

function
[species,err,SI,solids]=NR_method(Asolution,Asolid,Ksolid,Ksolution,T,
guess,iterations,criteria)

Nx=size(Asolution,2); Ncp=size(Asolid,2); Nc=size(Asolution,1);
X=guess;
```

```
for II=1:iterations

    Xsolution=X(1:Nx); Xsolid=[]; if Ncp>0; Xsolid=X(Nx+1:Nx+Ncp); end

    logC=(Ksolution)+Asolution*log10(Xsolution); C=10.^(logC); % calc
species

    if Ncp>0;
        Rmass=Asolution'*C+Asolid*Xsolid-T;
    end


    if Ncp==0; Rmass=Asolution'*C-T; end % calc residuals in mass
balance

    Q=Asolid'*log10(Xsolution); SI=10.^(Q+Ksolid);
    RSI=ones(size(SI))-SI;

    % calc the jacobian

    z=zeros(Nx+Ncp,Nx+Ncp);

    for j=1:Nx;
        for k=1:Nx;
                for i=1:Nc;
z(j,k)=z(j,k)+Asolution(i,j)*Asolution(i,k)*C(i)/Xsolution(k); end
        end
    end

    if Ncp>0;
    for j=1:Nx;
        for k=Nx+1:Nx+Ncp;
                t=Asolid';
                z(j,k)=t(k-Nx,j);
        end
    end
```

```
    end

    if Ncp>0
    for j=Nx+1:Nx+Ncp;
        for k=1:Nx
              z(j,k)=-1*Asolid(k,j-Nx)*(SI(j-Nx)/Xsolution(k));
        end
    end
    end

    if Ncp>0
    for j=Nx+1:Nx+Ncp
        for k=Nx+1:Nx+Ncp
            z(j,k)=0;
        end
    end
    end

    R=[Rmass; RSI]; X=[Xsolution; Xsolid];

    deltaX=z\(-1*R);
    %deltaX=-1*inv(z)*(R);
    one_over_del=max([1, -1*deltaX'./(0.5*X')]);
    del=1/one_over_del;
    X=X+del*deltaX;

    %X=X+deltaX;

    tst=sum(abs(R));
    if tst<=criteria; break; end

end

logC=(Ksolution)+Asolution*log10(Xsolution); C=10.^(logC); % calc
species
RSI=ones(size(SI))-SI;
```

```
if Ncp>0; Rmass=Asolution'*C+Asolid*Xsolid-T; end % calc residuals in
mass balance
if Ncp==0; Rmass=Asolution'*C-T; end % calc residuals in mass balance

err=[Rmass];

species=[C];
solids=Xsolid;

end

% ----------- NR method just solution species

function
[species,err,SI]=NR_method_solution(Asolution,Asolid,Ksolid,Ksolution,
T,guess,iterations,criteria)

Nx=size(Asolution,2); Ncp=size(Asolid,1); Nc=size(Asolution,1);
X=guess;

for II=1:iterations

   Xsolution=X(1:Nx);

   logC=(Ksolution)+Asolution*log10(Xsolution); C=10.^(logC); % calc
species

   Rmass=Asolution'*C-T;

   Q=Asolid*log10(Xsolution); SI=10.^(Q+Ksolid);
   RSI=ones(size(SI))-SI;

   % calc the jacobian

   z=zeros(Nx,Nx);

   for j=1:Nx;
```

```
        for k=1:Nx;
              for i=1:Nc;
z(j,k)=z(j,k)+Asolution(i,j)*Asolution(i,k)*C(i)/Xsolution(k); end
        end
    end

    R=[Rmass]; X=[Xsolution];

    deltaX=z\(-1*R);
    %deltaX=-1*inv(z)*(R);
    one_over_del=max([1, -1*deltaX'./(0.5*X')]);
    del=1/one_over_del;
    X=X+del*deltaX;

    %X=X+deltaX;

    tst=sum(abs(R));
    if tst<=criteria; break; end

end

logC=(Ksolution)+Asolution*log10(Xsolution); C=10.^(logC); % calc
species
RSI=ones(size(SI))-SI;

Q=Asolid*log10(Xsolution); SI=10.^(Q+Ksolid);
RSI=ones(size(SI))-SI;

Rmass=Asolution'*C-T;

err=[Rmass];

species=[C];

end
```

```
% ----- equilib definition ----------------

function
[KSOLUTION,KSOLID,ASOLUTION,ASOLID,SOLUTIONNAMES,SOLIDNAMES]=get_equil
ib_defn;

%%%%%%%%%%%%%%%%%%%%%%%%%%%%%%%%%%%%%%%%%%%%%%%%%%%%%%%%%%%%%%%%%%%%%%%%
%%%%%%%%%%%%%
%H+ TiOH  S2 PO4 logK  species name
Tableau=[...
1   0   0 0 0       {'H'}
0   1   0 0 0       {'TiOH'}
0   0   0 1 0       {'PO4'}
0   0   1 0 0       {'S2'}
-1  0   0 0 -14     {'OH'}
1   1   0 0 3.9     {'TiOH2'}
-1  1   0 0 -8.7    {'TiO'}
1   0   0 1 11.66   {'HPO4'}
2   0   0 1 18.64   {'H2PO4'}
3   0   0 1 20.65   {'H3PO4'}
1   0   1 1   14.3    {'TiOPO3'}
2   2   0 1   25.1    {'TiO2PO2'}
3   2   0 1   29.6    {'TiO2POOH'}
];


%   H+  TiOH    PO43-   Log K
% TiOH+ 1   1   0   3.9
% TiO-  -1  1   0   -8.7
% HPO42-    1   0   1   11.66
% H2PO4-    2   0   1   18.64
% H3PO4 3   0   1   20.65
% TiOPO3    1   1   1   30.3
% TiO2PO2   2   1   1   22.1
% TiO2POOH  3   1   1   15.6
```

```
%%%%%%%%%%%%%%%%%%%%%%%%%%%%%%%%%%%%%%%%%%%%%%%%%%%%%%%%%%%%%%%%%%%%%%%%%%%%
%%%%%%%%%%

n=size(Tableau,2);
ASOLUTION=cell2mat(Tableau(:,1:n-2));
KSOLUTION=cell2mat(Tableau(:,n-1));
SOLUTIONNAMES=strvcat(Tableau(:,n));

% -------------- solid values
%H+ M  Cl logK  species name
%%%%%%%%%%%%%%%%%%%%%%%%%%%%%%%%%%%%%%%%%%%%%%%%%%%%%%%%%%%%%%%%%%%%%%%%%%%%55
STableau=[...
-2  1   0 0 -120.56    {'dummy'}
];
%%%%%%%%%%%%%%%%%%%%%%%%%%%%%%%%%%%%%%%%%%%%%%%%%%%%%%%%%%%%%%%%%%%%%%%%%%%%

ASOLID=cell2mat(STableau(:,1:n-2));
KSOLID=cell2mat(STableau(:,n-1));
SOLIDNAMES=strvcat(STableau(:,n));

end

% ----------- for fixed pH ----------------

function
[Ksolution,Ksolid,Asolution,Asolid]=get_equilib_fixed_pH(KSOLUTION,KSO
LID,ASOLUTION,ASOLID,pH)

    [N,M]=size(ASOLUTION);
    Ksolution=KSOLUTION-ASOLUTION(:,1)*pH;
    Asolution=[ASOLUTION(:,2:M)];
    [N,M]=size(ASOLID);
    Ksolid=KSOLID-ASOLID(:,1)*pH;
    Asolid=[ASOLID(:,2:M)];
 end
```

A.2. MATLAB™ script used to simulate experimental data to fit into Freudlich isotherm model.

```
 function II=Freundlich_pH5_isotherm_PO4_on_Tio2_CaptainChoi
clear; Figure(1); clf

PT=[0.25    0.5 0.9 1.925   2.939   3.981   5   6.07    6.99 100.94]; % mg
P/L
boundP=[0.068686869 0.265306122 0.458823529 0.617142857 0.750515464
0.696296296 0.836363636 0.919587629 0.837037037 0.983256]; % mg P/L

boundP=(boundP);
PT=(PT);
residualP=PT-boundP;

semilogx((PT),boundP,'ko','markersize',10,'markerfacecolor','r')
set(gca,'linewidth',2,'fontsize',14)
xlabel('[PO_4^{3-}] (mg/L)','fontsize',14)
ylabel('bound P (mg/L)','fontsize',14)
free=PT;
hold on;

options=optimset('fminsearch');
options=optimset(options,'Display','iter','MaxIter',1000,'TolX',1e-
4,'Tolfun',1e-4);

p0=[-5 log10(1.1)];


K=10.^p0(1); n=10.^p0(2);
logfreeplot=-5:0.001:2.2; freeplot=10.^logfreeplot;
modelguess=(K.*freeplot.^(1./n));

hold on;
```

```
bestfitp = fminsearch(@(p) freundlich(p,free,boundP), p0, options);

bestfitp

K=10.^bestfitp(1); n=10.^bestfitp(2);
model=(K.*freeplot.^(1./n));
hold on;

semilogx(freeplot,model,'k','linewidth',2)
axis([10^(-5) 10^(5) 0 1.2])

II=-1;

end

function II=freundlich(p,free,boundP)

K=10.^p(1); n=10.^p(2);
model=(K.*free.^(1./n));
residual=boundP-model;
II=log10(sum((residual.^2)));

end
```

A.3. MATLAB™ script used to simulate experimental data to fit into Langmuir isotherm model.

```
function II=simple_pH5_isotherm_PO4_on_TiO2
clear; Figure(1); clf

PT=[0.25   0.5 0.9 1.925   2.939   3.981   5   6.07    6.99 100.94]; %
mg P/L

bound=[0.068686869  0.265306122 0.458823529 0.617142857 0.750515464
0.696296296 0.836363636 0.919587629 0.837037037 0.983256]; % mg/g

semilogx((PT),bound,'ko','markersize',8,'markerfacecolor','g')

set(gca,'linewidth',2,'fontsize',14)
xlabel('[PO_4^{3-}] (mg/L)','fontsize',14)
ylabel('bound P (mg/g)','fontsize',14)
free=PT;

options=optimset('fminsearch')
options=optimset(options,'Display','iter','MaxIter',1000,'TolX',1e-
4,'Tolfun',1e-4)

p0=[-0.1065 -0.5844];
bestfitp = fminsearch(@(p) Langmuir(p,free,bound), p0, options);

bestfitp

K=10.^bestfitp(1); LT=10.^bestfitp(2);
logfreeplot=-8:0.0001:5; freeplot=10.^logfreeplot;
model=(LT*K*freeplot)./(K*freeplot+1);

hold on;

semilogx(freeplot,model,'k--','linewidth',2)
axis([10^(-5) 10^(5) 0 1.2])
```

```
II=-1;

end

function II=Langmuir(p,free,bound)

K=10.^p(1); LT=10.^p(2);
model=(LT*K*free)./(K*free+1);
residual=bound-model;
II=log10(sum((residual.^2)));

end
```